

Bio-Inspired Synthesis of Gold Nanoparticles Using Leaf Extract of *Jamun* and Research on Its Biomedical Potential

Gitishree Das¹, Han-Seung Shin², Kyung-Jik Lim², Jayanta Kumar Patra¹

¹Research Institute of Integrative Life Sciences, Dongguk University-Seoul, Goyangsi, Republic of Korea; ²Department of Food Science & Biotechnology, Dongguk University-Seoul, Goyangsi, Republic of Korea

Correspondence: Jayanta Kumar Patra, Research Institute of Integrative Life Sciences, Dongguk University-Seoul, Goyangsi, 10326, Republic of Korea, Email jkpatra@dongguk.edu

Background: Bio-based synthesis of metallic nanoparticles has garnered much attention in recent times owing to their non-toxic, environmentally friendly, and cost-effective nature.

Methods: In this study, gold nanoparticles (S4-GoNPs) were synthesized by a simple and environmentally friendly technique using an aqueous extract of jamun leaves (JLE) as an effective capping, stabilizer, and reducing agent. JLE was screened for the presence of phytochemicals followed by synthesis, characterization, and evaluation of their antibacterial, antidiabetic, antioxidant, and photocatalytic degradation potentials using standard established procedures.

Results: The phytochemical profile of JLE was found to be rich in flavonoids, tannins, terpenoid phenols, anthraquinones, and cardiac glycosides. Its GC-MS analysis revealed the presence of compounds majorly of them as the (1R)-2,6,6-Trimethylbicyclo[3.1.1]hept-2-ene (5.141%), 2(10)-pinene (4.119%), α -cyclopene (5.274%) α , α -muurolene (7.525%), naphthalene, 1,2,3,4,4a,5,6,8a-octahydro-7-methyl-4-methylene-1-(1-methylethyl)-(1.alpha.,4a.beta.,8a.alpha) (8.470%), delta-cadinene (23.246), α -guajene (3.451%), and gamma-muurolene (4.379%). The visual morphology and UV-Vis spectral surface plasmon resonance at 538 nm confirmed the successful synthesis of S4-GoNPs. The average particle size was determined as 120.5 nm with Pdi = 0.152, and -27.6 mV zeta potential. Using the Scherrer equation, the average crystallite size was calculated as 35.69 nm. S4-GoNPs displayed significant antidiabetic properties, with 40.67% of α -amylase and 91.33% of α -glucosidase inhibition activity. It also exhibited promising antioxidant potential in terms of the DPPH (91.56%) ABTS (76.59%) scavenging. It displayed 31.04% tyrosinase inhibition at 0.1 mg/mL. Moreover, it also demonstrated encouraging antibacterial effects with zones of inhibition ranging from 11.02 – 14.12 mm as compared to 10.55–16.24 mm by the reference streptomycin (at 0.01 mg/disc). In addition, S4-GoNPs also showed potential for the photocatalytic degradation of the industrial dye, methylene blue.

Conclusion: In conclusion, these results suggest the promising applicability of green-synthesized S4-GoNPs in various sectors, including the biomedical, cosmetic, food, and environmental waste management industries.

Keywords: gold nanoparticles, antidiabetic, antioxidant, antibacterial, tyrosinase inhibition

Introduction

Nanotechnology is an emerging field with incredible development in nanoparticle applications for countless scientific and high-tech applications in various fields such as electronics, biomedical, biosensing, food sector industry, clothing, cosmetics, and therapeutics.¹⁻³ Nanomaterials with nanoscale size ranges and large volume ratios have acquired more effective physical and chemical properties than their macroforms.^{3,4} A series of inventions related to nanotechnology resulted in the production of numerous nano-dimensional materials at the industrial scale.^{5,6} Further, it is believed that the use of nanomaterials will increase in the everyday life and thus it is essential that these nano materials could be able to establish suitable interactions with various biomolecules and bioactive compounds, both within and on the cell surfaces.⁶ A report by, Vance et al,⁷ stated that approximately 1814 nano-based products are available in the market globally for the consumers to use. Moreover, the market share of the nano-

based materials is increasing day by day was estimated at USD 79.14 billion in the year 2023 (<https://www.fortunebusinessinsights.com/nanotechnology-market-108466>).

Nanomaterials can be synthesized using various physical, chemical, and biological forms.² It has been proven that although the chemical method of nanoparticle synthesis is highly productive, however, it is not effective as it gives rise to a high quantity of hazardous byproducts, low biocompatibility, and involves high cost.^{2,3,8,9} In contrast, the biological synthesis method is more operative and safe, and attains a superior yield along with environmental friendliness, reduced reagent requirements, and low cost.^{2,3,9,10} The defensible biosynthesis of noble metal nanoparticles has attracted substantial attention because it uses standard temperature and pressure for the manufacture of nanomaterials, which saves a noteworthy amount of energy and money.^{11,12} The biological method of nanoparticle synthesis, most commonly called the green synthesis method, involves the use of various biological sources, such as bacteria, fungi, algae, and plants, as reducing and stabilizing agents in the synthesis process.^{9,11,13} All of these reducing agents are economically sustainable and environment-friendly.¹⁴ Of all the biological sources, plant part (such as the leaf, stem, root, and seeds) extracts are considered more suitable because of their easy availability, easy handling, rich bioactive compounds, safe, and large-scale production.^{9,15} Plant extracts are rich in numerous bioactive compounds with medicinal values that can be incorporated into synthesized nanoparticles, and their potential can be enhanced.¹⁶ Plant extracts contain numerous bioactive compounds that have beneficial effects on the reduction and stabilization of nanoparticles.¹⁷ The bioactive compounds present in plants and their extracts act as reducing, precipitating, and capping agents, thus substantially influencing the shape, size, and other key features of nanoparticles.^{3,18} Plant-based biosynthesis of nanomaterials is considered the most acceptable method because of its relatively mild, environmentally friendly, and lucrative properties.¹⁹ It has been already proven that plant extracts are rich in a number of bioactive compounds including proteins, carbohydrates, phenols, flavanols, terpenoids, vitamins, etc.¹⁹ These constituents play a major role in bioreduction, capping, and stabilization of the synthesized nanomaterials. Plant extract-mediated gold nanoparticles (GoNPs) deliver enhanced properties as compared to the chemically produced GoNPs.²⁰

Metallic nanomaterials have attracted attention because of their applications in diverse fields, including electronics, biomedical, chemical and biological sensors, drug delivery, food packaging, cosmetics, and many more.²¹ These nanoparticles, because of their small size and high loading capacities, can augment the solubility of herbal medications, thereby administering at the exact affected target area in the body, resulting in greater accuracy and better performance.²² Modification of nanoparticles into various forms has allowed the desired therapeutic agents to defeat the biological obstructions, single out the molecular changes, and take part as a moderator in the process of molecular interactions.²³ These nanoparticles may be engaged in directing a natural bioactive component into the exact location of the affected organ, thus enlightening the drug delivery mechanism, choosiness, effectiveness, and protection of the organ, along with the application of lower doses of medications.²⁴ Considering the vast potential of nanomaterials in biomedical fields such as drug delivery, cancer therapies, and antimicrobial targets, there is increasing interest in nanomaterial research and applications. Recently, a number of nanoparticles, such as palladium, gold, silver, and platinum, have been widely tested on the human body.^{3,9,11,19,22,24} However, because of their unique properties such as versatility, inertness, biocompatibility, and optical, thermal, catalytic, optical-electronic controllable properties and surface modifiability, gold nanoparticles (GoNPs) have been considered the most accepted metal nanoparticles for biomedical applications.^{19,20,22,25–27}

Furthermore, because of their well-defined surface chemistry, GoNPs can be easily conjugated with diverse compounds and molecules, and are not harmful to humans at low doses.²⁶ In addition, GoNPs exhibit antibacterial, antioxidant, antidiabetic, and catalytic properties.^{3,22,28,29} It has been reported that the synthesis and stability of GoNPs require both capping and reducing agents, and in most cases, synthetic chemicals such as sodium borohydride, hydrazine, and surfactants are typically used in the synthesis process.^{19,20} However, these synthetic chemical reactions require input energy and must be removed properly after the completion of the reaction process to avoid any toxicity issues in its biomedical use.¹⁹ To overcome this issue, the one-pot green synthesis method for gold nanoparticle synthesis using plant material is a reliable and best alternative process.

Syzygium cumini Lam. (commonly called Jamun) is an evergreen tropical tree that belongs to the Myrtaceae family. It has many local names such as black plum, java plum, jambolao (Brazil), Indian berry, damson, etc.^{30,31} All parts of this plant, such as the seeds, berries, leaves, and bark, are used for medicinal purposes.^{32,33} Its leaves are acknowledged as an important source

of phytochemicals such as tannins, phenolic acids, flavonoids, and terpenoids.³⁴ Polyphenols are considered the major constituents of Jamun leaves.³⁴ Shidiki and Vyas³⁵ have identified 20 compounds such as caffeic acid, 3-(3-hydroxy phenyl) propionic acid, xanthoxylin, ferulic acid, quinic acid, diferulic acid, methyl gallate, gallic acid, astragalol, cianidanol, butin, kaempferide, 4'-hydroxyflavan, taxifolin, isoquercetin, 3,5,7,4'-tetrahydroxy-6-(3-hydroxy-3-methylbutyl) flavone; cedrol, 6-O-feruloyl-D-glucose, palmitic acid, and punicic acid from the aqueous leaf extracts of *S. cumini* by Liquid chromatography–mass spectrometry (LC-MS) as shown in [Supplementary Table 1](#). Furthermore, a few other authors have also identified a number of bioactive compounds from the aqueous extract of *S. cumini* leaves using a number of analytical techniques, including high-performance liquid chromatography, liquid chromatography, and nuclear magnetic resonance spectroscopy, the details of which are presented in [Supplementary Table 2](#).

In addition, these parts are used for the treatment of various ailments. The ash of Jamun leaves has been used for strengthening teeth and gums.³⁶ A decoction of the stem bark and leaves of jamun was used to subside the smell of the armpit.³⁷ Jamun leaves are considered to support liver health and aid the detoxification process.³⁴ Jamun leaves have been reported to be consumed daily by cooking them in water to cure diabetes.³⁰ Leaf juice has been used as an antidote for opium poisoning, and oral intake of the leaves for a few days has been reported to be beneficial in reducing jaundice in human beings.³⁸ Many uses such as antidiabetic, antioxidant, anticancer, antimicrobial, astringent, diuretic, blood strengthener, anti-inflammatory, anti-HIV, anthelmintic, gastroprotective, etc, have been reported for this plant and its parts.^{31,32,38} It is rich in alkaloids, flavonoids, glycosides, polyphenols, tannins, terpenes, anthraquinones, essential oils, etc.^{39,40} Further, there are a few reports on the use of JLE in the biosynthesis of different types of nanoparticles and their application in various fields.^{2,31,41,42} Taken together, it is assumed that the vast resource of bioactive compounds in the jamun tree and its parts is followed by numerous medicinal values and properties as evident from previously published literature, and it is assumed that if this plant part is extracted and its extract is used in the gold nanoparticles (GoNPs) synthesis, then the bioactive compounds present could enhance the activity of the GoNPs by synergistic effects, thereby resulting in improved biological potential of the GoNPs. Considering this, in the current research, the synthesis of gold nanoparticles has been undertaken using the jamun leaf aqueous extract and the investigation of its biological potential in terms of its antioxidant, antidiabetic, antibacterial activity, and photocatalytic degradation of industrial dyes have been attempted.

Materials and Methods

Reagents and Chemicals

All solvents and chemicals were of analytical grade and purchased from Sigma Aldrich, USA, and Daejung Chemicals, Korea. All the reagent solutions were prepared using deionized water.

Jamun Leaf Extract Preparation and Phytochemical Analysis

Fresh leaves of the *S. cumini* Lam. (commonly called Jamun), collected from the botanical garden of Dongguk University ([Figure 1A](#)), were authenticated by the botanical specialist, and a herbarium specimen was prepared and recorded (RIILSEH No. 202211–05) at Dongguk University. Fresh leaves were washed to remove dirt and dust particles, dried, and cut into small pieces, followed by drying at room temperature for 10 days. After 10 d, the leaves were ground into a powder using an electric grinder. Then, 50 g of powdered Jamun leaves (JE) was put in 500 mL of the flask with 250 mL of sterile distilled water, followed by boiling for 15 min to prepare the Jamun leaf extract (JLE). The JLE was cooled to ambient temperature, filtered, and stored in a refrigerator. The presence of various phytochemicals (tannins, saponins, flavonoids, phenols, carbohydrates, terpenoids, proteins, amino acids, anthraquinones, and cardiac steroidal glycosides) in JLE has been investigated using standard referred protocols.^{43,44} The Gas chromatography–Mass Spectrometry (GC–MS; Agilent Technologies, Inc., USA, 7820A/5975C MSD, GC System and DANI Headspace auto-sampler, DANI Analytica SRL, MI, Italy) was used for the analysis of JLE as per standard established protocol. An HP-5ms Ultra Inert column containing (5%-phenyl)-methylpolysiloxane (30m × 0.25 mm i.d., 0.25 μm film thickness; J & W Scientific, Agilent) was used as the stationary phase and helium as the carrier gas (at a flow rate of 0.8 mL/min), and a mass-selective detector was operated in electron impact ionization mode at 70 eV in the scanning range of m/z 50–550. Integration parameters as autoint1.e and ChemStation as integrators and MassHunter software were used for this purpose.

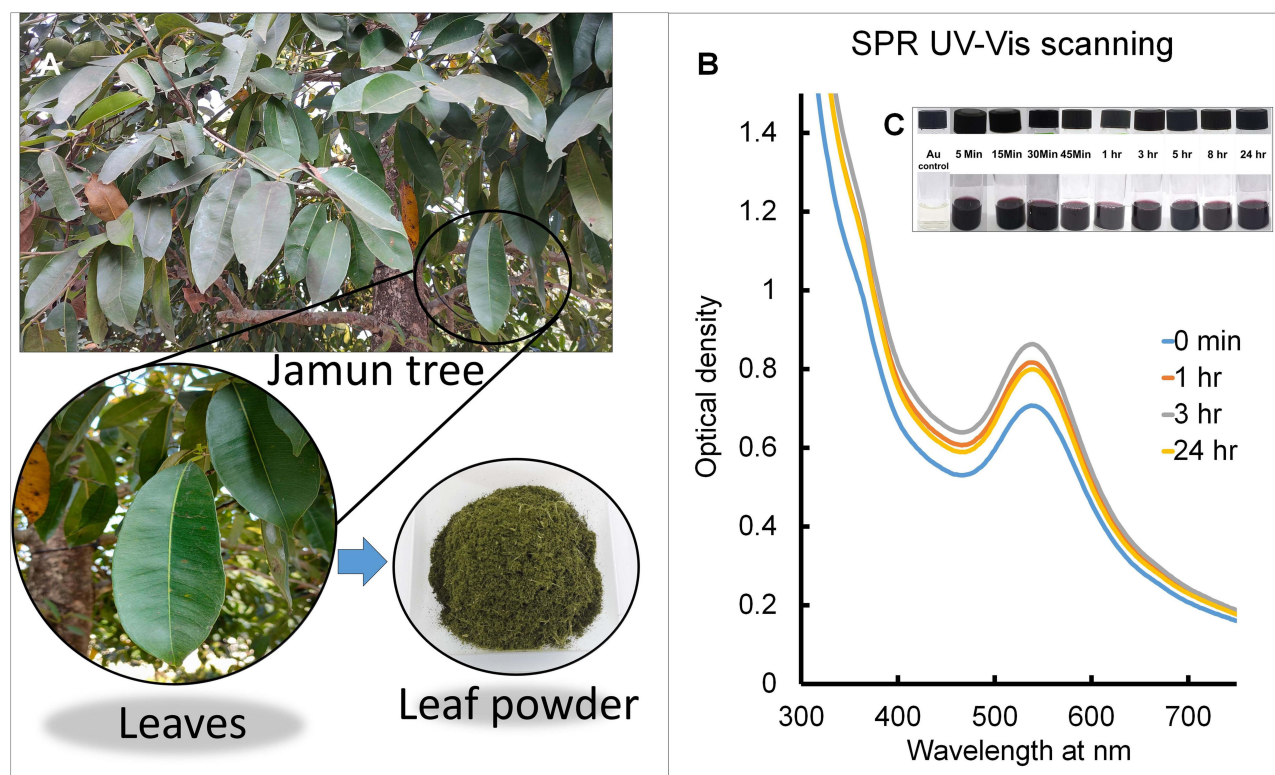


Figure 1 (A) Photos of Jamun tree and jamun leaf powder; (B) SPR UV-VIS scanning of S4-GoNPs at regular time intervals; (C) visual color changes with time.

The National Institute of Standards and Technology (NIST) library was used for precise identification of the bioactive phytochemicals present in JLE.

Production of GoNPs by JLE and Its Characterizations

For the green synthesis of GoNPs, JLE extract was used as a reducing, capping, and stabilizing agent. Briefly, approximately 100 mL of $\text{HAuCl}_4 \cdot 3\text{H}_2\text{O}$ was taken in a 0.5 L flat bottom flask, and approximately 10 mL of JLE was added dropwise with continuous stirring at ambient temperature. The synthesis of GoNPs (S4-GoNPs) was monitored visually, followed by UV-VIS spectral scanning from 300 to 750 nm at every 2 nm interval for 24 h at regular time intervals. Following the confirmation of biological synthesis, the S4-GoNPs solution was centrifuged at 12,000 rpm for 20 min together with 3–4 distilled water washes to remove the unattached compounds from the JLE. The dried S4-GoNPs were collected in powder form after drying at room temperature in an oven for further characterization. Following biosynthesis, S4-GoNPs were subjected to various morphological, chemical, and physical characterizations according to the prescribed standardized methodology.⁴⁵ The nature and elemental composition of the S4-GoNPs were examined by scanning electron microscopy (SEM) and energy-dispersive X-ray spectroscopy (EDS) machine connected to it. In addition, the surface characteristics were studied using atomic force microscopy (AFM). The crystalline structure was characterized using X-ray diffraction (XRD) analysis. The zeta potential and the particle size of green-synthesized S4-GoNPs were assessed using a zeta potential machine. The Thermogravimetric (TGA) instrument estimated the composition and thermal stability of the green synthesized S4-GoNPs from 20°C to 900°C at every 10°C/minute ramping time. Finally, the functional group composition of both JLE and S4-GoNPs was estimated using a Fourier transform infrared spectrophotometer (FTIR) between 4000 and 400 cm^{-1} .

Assessment of the Biomedical Activities of S4-GoNPs

The biomedical properties of green-synthesized S4-GoNPs were explored using the well-recognized antibacterial, antidiabetic, antioxidant, and tyrosinase inhibition potentials. The antibacterial action of S4-GoNPs was investigated

using a standard disc diffusion assay against seven foodborne pathogenic bacteria, out of which four are Gram negative: *Aeromonas hydrophila* ATCC 7966, *Escherichia coli* O157:H7 ATCC 23514, *Salmonella* Typhimurium KCTC 1925, and *Pseudomonas aeruginosa* ATCC 27583; and three Gram positive: *Enterococcus faecium* DB01, *Pediococcus* sp., and *Bacillus cereus* KCTC 3624.⁴⁶ Briefly, S4-GoNPs (100 µg/disc) and streptomycin (10 µg/disc) were seeded on culture plates spread with the pathogenic bacteria and incubated at 37 °C for 1 d, followed by a measurement of the diameter of the zone of inhibition around the disc. The minimum inhibitory concentration (MIC) and minimum bactericidal concentration (MBC) of both S4-GoNPs and streptomycin (positive reference control) were determined using well-established two-fold dilution methods. The MIC was determined by visual surveillance after a 1-day gestation period and compared with that of control tubes containing only liquid broth media. The minimal S4-GoNPs/streptomycin concentrations with no visual growth of pathogens were considered the MIC values, whereas minimal concentrations that showed no growth in the culture plates were considered the MBC values.

The antidiabetic effects of S4-GoNPs were determined using α -amylase and α -glucosidase enzyme inhibition assays. The α -amylase inhibition potential of S4-GoNPs was investigated following previously used processes with limited adjustments.^{47,48} Acarbose was taken as a reference-positive control for the experiment. In brief, the tested materials (40 µL, at different concentrations of 0.01 g/1000 µL of dimethyl sulfoxide) were again prepared in 160 µL of 20 mM phosphate buffer saline (pH 6.9), including 0.0067 M sodium chloride in 2 mL bottles, and incubated for 300 s with 200 µL of 4 U/mL α -amylase prepared in ice-cold distilled water. The start of the reaction process was instigated by adding 0.4 mL of soluble potato starch mixture in phosphate buffer saline. After 3 min incubation, trailed by mixing of 0.4 mL of DNS color reagent and heating for 10 min at 90°C in the water bath and subsequent cooling. Approximately 50 µL of the test material was diluted with another 175 µL of water, and the absorbance was measured at 540 nm using a spectrophotometer. Enzyme activity was calculated using Equation 1.

$$\text{Inhibition/Percentage scavenging} = \frac{K_{OD} - T_{OD}}{K_{OD}} \times 100 \quad (1)$$

Where K_{OD} is the OD of the control, and T_{OD} is the OD of the treatment.

Similarly, the α -glucosidase inhibition potential of S4-GoNPs was investigated following earlier regular processes with limited adjustments.⁴⁸ One milliliter of the reaction test material contained S4-GoNPs and acarbose (reference-positive control) at three concentrations (25–100 µg/mL), 4 units/mL of α -glucosidase enzyme, and potassium phosphate buffer at pH 6.8, and was incubated for 10 min. About 100 µL of 3 mM p-nitrophenyl- α -d-glucopyranoside was used as the substrate and the test material was further incubated for another 20 min at 37°C. After completion of the incubation period, 2 mL of Na₂CO₃ was added to the test material, the optical density (OD) was measured at 405 nm, and enzyme activity was determined using the following equation 1.

Next, the antioxidant effects of the S4-GoNPs were estimated using three different assays, namely DPPH (1,1-diphenyl-2-picrylhydrazyl) radical scavenging, ABTS [2,2-azinobis(3-ethylbenzothiazoline-6-sulfonic acid)] radical scavenging, and reducing power assays. The DPPH assay was performed as described by Patra et al.⁴⁹ Three different concentrations (25–100 µg/mL) of S4-GoNPs and gallic acid (reference-positive control) were used in the experiment. The optical density was determined at 517 nm using a multiplate reader, and the scavenging percentage was calculated using Equation 1. Similarly, for the ABTS assay, the standard protocol of Das et al.⁴⁵ was followed using three different concentrations (25–100 µg/mL) of S4-GoNPs and gallic acid (reference-positive control). The OD values were determined at 734 nm using a multiplate reader, and the scavenging percentage was calculated using Equation 1. The reducing power assay was performed according to the protocol of Das et al.⁴⁵ with three different concentrations (25–100 µg/mL) of S4-GoNPs and gallic acid (reference-positive control). The resulting OD values were recorded at 700 nm. The effective concentration that showed 50% of activity (IC₅₀/IC_{0.5} value) was calculated from the graph. The tyrosinase inhibition potential of S4-GoNPs was investigated using the protocol described by Das et al.⁴⁵ For this experiment, three different concentrations (25–100 µg/mL) of S4-GoNPs and Kojic acid (reference-positive control) were used, and the OD values were obtained at 475 nm, followed by the calculation of the inhibition potential using Equation 1.

Assessment of Photocatalytic Degradation of Methylene Blue Industrial Dye

The photocatalytic degradation effects of S4-GoNPs against methylene blue industrial dye were investigated following a standard protocol with minimal modifications.^{50,51} The degradation of the industrial dye was monitored at regular time intervals by measuring the OD values in the 300–900 nm range, and the percentage degradation was calculated using the following equation:

$$\text{Dye degradation \%} = \frac{OD_{bl} - OD_{al}}{OD_{bl}} \times 100 \quad (2)$$

where OD_{bl} , is the OD of the dye solution before light contact and OD_{al} is the OD of the dye solution after light contact.

Statistical Investigation of the S4-GoNPs

Experiments were conducted thrice, and the data were interpreted as mean values with standard deviations. One was the analysis of variance; Duncan's multiple range test at $P < 0.05$; Pearson's correlation, regression analysis, and other calculations were performed using SPSS (version 27.0; IBM Corp., Armonk, NY, USA) and OriginPro 2024 version 10.1.

Results and Discussion

In the current study, the leaves of the Jamun tree (Figure 1A) were selected, and their aqueous extracts were prepared for biomediated green synthesis of GoNPs. Prior to the synthesis, a preliminary phytochemical profile of the aqueous JLE was undertaken, and the leaf extract was found to be rich in a number of phytochemicals, such as flavonoids, tannins, terpenoid phenols, anthraquinones, and cardiac glycosides (Table 1). The presence of these phytochemicals has also been reported in previous publications.^{52–57} A study by Prabhakaran et al⁵⁸ has also shown the presence of carbohydrates, saponins, tannins, and phenols in jamun leaf extracts. In another study, Bari et al⁵⁷ have highlighted the presence of flavonoids, saponins, tannins, and phenols in aqueous jamun leaf extracts. Phenolic compounds play a key role in human health by reducing the risk and preventing the growth of some deteriorating diseases, such as cancer, cardiovascular diseases, and diabetes, as well as by combating antioxidant and anti-inflammatory processes.^{59,60} Further, there is evidence that the leaves of the Jamun tree are rich in a number of compounds including betulinic acid, quercetin, α -pinene, β -sitosterol, α -cadinol, α -terpeneol, L-limonene, eucarvone, α -bornyl acetate, caryophyllene, α -terpineol, and many more.^{55,56,61–64} A study by Dan et al⁶⁵ has reported on the quantitative phytochemical prospective of jamun leaf extracts, accounting for 2.05–6.15 mg/g and 1.5–7.5 mg/g of alkaloids and proteins, respectively. In another review, the author reported the presence of 9.1% protein, 4.3% fat, and 17% of fiber in the Jamun leaf.⁵⁶


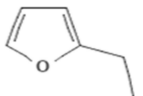
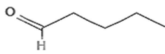
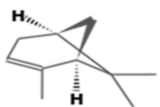
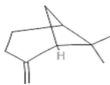
Further characterization of JLE was carried out by gas chromatography-mass spectrometry (GC-MS) analysis, and the number of compounds and their percentages are presented in Table 2. The GC-MS analysis of the JLE revealed the presence of a number of compounds, majorly of them as the (1R)-2,6,6-Trimethylbicyclo[3.1.1]hept-2-ene (5.141%), 2 (10)-pinene (4.119%), α -cyclopene (5.274%) α , α -muurolene (7.525%), naphthalene, 1,2,3,4,4a,5,6,8a-octahydro-7-methyl-4-methylene-1-(1-methylethyl)-(1.alpha.,4a.beta.,8a.alpha) (8.470%), delta-cadinene (23.246), α -guajene (3.451%), and gamma-muurolene (4.379%) (Table 2). Many of the detected active compounds possessed substantial pharmacological activities, the details of which are discussed below. The medicinal potential and biological activities of the identified compounds are shown in Supplementary Table 3. α - and β -pinenes are monoterpenes with numerous pharmacological properties, such as antimicrobial, antioxidant, antimalarial, anti-inflammatory, anti-nociceptive, anticancer properties, etc.^{64,66–70} Copaene (α -copaene) is commonly found in essential oils of many plants^{71,72} and has numerous medicinal properties such as antioxidants and antigenotoxicity.⁷³ (+)-Alpha-muurolene is a natural compound found in some plants with medicinal properties.^{74,75} Plants rich in compounds such as naphthalene, 1,2,3,4,4a,5,6,8a-octahydro-7-methyl-4-methylene-1-(1-methylethyl)-(1.alpha.,4a.beta.,8a.alpha) have been reported to have anticancer, antimicrobial, and antioxidant potential.^{76,77} δ -Cadinene is one of the most extensively occurring plant sesquiterpenes, with numerous medicinal properties, including treatment against rheumatic disorders and antimicrobial and antioxidant properties.^{78–81} Azulene (1,2,3,4,5,6,7,8-octahydro-1,4-dimethyl-7-(1-methylethenyl)-, (1S,4S,7R)-) is a natural product found in many plants. It has a number of biological properties, including anti-inflammatory, antimicrobial, antineoplastic,

Table 1 Phytochemical Analysis of Aqueous JLE

Phytochemicals	Aqueous JLE
Tannin	+
Flavonoids	+
Terpenoids	+
Saponins	+
Phenol	+
Carbohydrates	+
Proteins & Amino acids	-
Anthraquinones	+
Cardiac steroidal glycoside	+

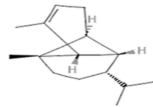
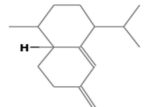
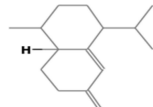
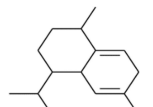
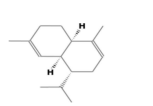
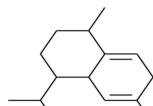
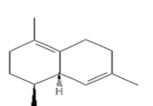
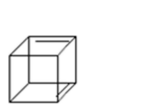
Notes: +, present; -, absent.

Table 2 GC-MS Analysis of Jamun Leaf Extract, Chemical Structure, and Percent Composition of the Major Compounds

No.	Retention Time	Compound Name	Chemical Formula	Mol Wtt. (g/mol)	Chemical Structure	Compound %
1.	2.161	2-Penten-1-ol, (Z)-	C ₅ H ₁₀ O	86.13		1.083
2.	2.295	Furan, 2-ethyl-	C ₆ H ₈ O	96.13		1.400
3.	3.337	Hexanal	C ₆ H ₁₂ O	100.16		2.897
4.	6.255	(1R)-2,6,6-Trimethylbicyclo[3.1.1]hept-2-ene; Cyclohexene, 1-methyl-4-(1-methylethenyl)-, (R)-; α-Pinene; Tricyclo[2.2.1.0 ^{2,6}]heptane, 1,7,7-trimethyl-; 2-Pinene; BICYCLO[3.1.1]HEPT-2-ENE, 2,6,6-TRIMETHYL-;	C ₁₀ H ₁₆	136.23		5.141
5.	7.569	2(10)-Pinene; Bicyclo[3.1.1]heptane, 6,6-dimethyl-2-methylene-, (1S)-	C ₁₀ H ₁₆	136.23		4.119

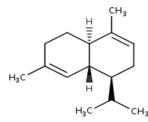
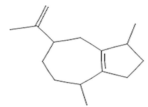
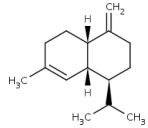
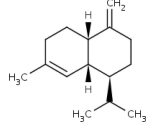
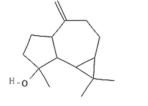
(Continued)

Table 2 (Continued).

No.	Retention Time	Compound Name	Chemical Formula	Mol Wtt. (g/mol)	Chemical Structure	Compound %
6.	23.961	Alfa-Copaene; Copaene	C ₁₅ H ₂₄	204.35		5.274
7.	27.506	(+)-epi-Bicyclosesquiphellandrene; cis-Muurolo-4(15),5-diene	C ₁₅ H ₂₄	204.35		1.5
8.	28.664	(+)-epi-Bicyclosesquiphellandrene	C ₁₅ H ₂₄	204.35		1.009
9.	28.828	Naphthalene, 1,2,3,4,4a,7-hexahydro-1,6-dimethyl-4-(1-methylethyl)-; CADINA-1,4-DIENE	C ₁₅ H ₂₄	204.35		1.389
10.	29.056	alpha.-Muurolole	C ₁₅ H ₂₄	204.35		7.525
11.	29.575	Naphthalene, 1,2,3,4,4a,5,6,8a-octahydro-7-methyl-4-methylene-1-(1-methylethyl)-, (1.alpha.,4a.beta.,8a.alpha.)-; Naphthalene, 1,2,4a,5,6,8a-hexahydro-4,7-dimethyl-1-(1-methylethyl)-	C ₁₅ H ₂₄	204.35		8.470
12.	29.975	delta.-Cadinene	C ₁₅ H ₂₄	204.35		23.246
13.	30.285	Cubenene	C ₈ H ₄	100.12		1.483

(Continued)

Table 2 (Continued).

No.	Retention Time	Compound Name	Chemical Formula	Mol Wtt. (g/mol)	Chemical Structure	Compound %
14.	30.491	Naphthalene, 1,2,4a,5,6,8a-hexahydro-4,7-dimethyl-1-(1-methylethyl)-, [1S-(1.alpha.,4a.beta.,8a.alpha.)]-;:alpha.-cadinene	C ₁₅ H ₂₄	204.35		1.694
15.	31.995	1,H-Dimethyl-7(1-hydroxy-1-methylethyl)[3,3a,4,5,6,7]hexahydro azulene; alpha-Guajene	C ₁₅ H ₂₄	204.35		3.451
16.	34.455	1-ISOPROPYL-7-METHYL-4-METHYLENE-1,2,3,4,4A,5,6,8A-OCTAHYDRONAPHTHALENE; gamma.-Muuroleone;	C ₁₅ H ₂₄	204.3511		4.379
17.	35.045	6.alpha.-Cadina-4,9-diene, (-)-;:gamma.-Muuroleone	C ₁₅ H ₂₄	204.3511		1.624
18.	36.630	1,1,7-TRIMETHYL-4-METHYLENEDECAHYDRO-1H-CYCLOPROPA[E]AZULENE	C ₁₅ H ₂₄ O	220.35		6.156

antidiabetic, and antiretroviral properties.^{82–84} Gamma-muuroleone is a sesquiterpene and a carbocyclic compound. 1,2,3,4,4a,5,6,8a-Octahydronaphthalene was substituted at positions 1, 4, and 7 with isopropyl, methylene, and methyl groups, respectively. It has been reported to possess anti-inflammatory, antinociceptive, and antioxidant properties.^{85,86} Similar compounds in the GC-MS profile of jamun leaf extracts have been reported previously.^{64,87} The medicinal potential of Jamun tree leaves has also been reported previously.^{30,56,88} Aqueous leaf extracts have been used in the treatment of diabetes.^{30,59} Leaf juice has been used as an antidote for opium poisoning and is effective in reducing jaundice³⁸ and dysentery.⁸⁸ Ahmed et al⁸⁹ have reported the anti-inflammatory, anti-coagulant, antioxidant, anti-proliferative, and analgesic potential of jamun leaf methanol extract. Because of the presence of these active compounds in the JLE, as evident from the GC-MS results (Table 2) and subsequent literature review, this extract could serve as a potential candidate for reducing, capping, and stabilizing agents in GoNP synthesis, and it could also enhance the biological potential of the synthesized S4-GoNPs. LC-MS analysis of the leaf extract of *S. cumini* as reported previously identified 20 different compounds, mainly phenolic and flavonoids (Supplementary Table 1),³⁵ which could have acted as reducing, capping, and stabilizing agents in the green synthesis of S4-GoNPs. Phytochemicals play a major role in the stabilization, size control, and minimization of agglomeration as well as the morphology of metal nanoparticles.⁹⁰ It has been reported that the rich bioactive compounds present in the plant extracts (in this case the JLE) (Tables 1, 2 and Supplementary Table 3), aid in the bioreduction of metal ions to nanoparticles by donating electrons to the metal ions, reducing them followed by stabilizing them in order to minimize the gathering of the nanoparticles.^{91,92} Besides, these phytochemicals also act as capping agents by forming a layer on the surface of the nanoparticles, as evident from various previous

publications.^{92–94} Furthermore, there are reports discussing that the presence of flavonoids, polyphenols, and proteins in the plant extracts are responsible for their role as a reducing agent in the biosynthesis of nanomaterials.^{92,93,95,96} A study by Zarzuela et al,⁹⁷ on the gold nanoparticles, have reported that the flavone sulfate molecules present in the plant extract mainly act as a reducing and stabilizing agent in the nanoparticle synthesis. Another report suggested that the interaction of bioactive compounds on the nanoparticle surface could be responsible for the stabilization of nanomaterials thereby enhancing their applications in various fields such as biomedical, sensors, etc.⁹⁸

After preliminary phytochemical screening, JLE was used as a reducing agent in the green synthesis of S4-GoNPs via a one-pot process. In the current case, an easy, one-pot synthesis method has been adopted for the synthesis of S4-GoNPs at normal temperature and neutral pH condition. It is known that the physical and chemical methods of synthesis of nanoparticles utilize various toxic chemicals and extremely harsh conditions,⁶ whereas in the bioinspired synthesis of S4-GoNPs, non-toxic chemicals and ambient temperature and pressure have been used that indicated an ecofriendly and cost-effective method of nanomaterial synthesis. A detailed schematic diagram describing the bioinspired synthesis of S4-GoNPs is presented in Figure 2, for a better understanding of the synthesis process. The possible mechanism of the biosynthesis involves the bioactive compounds from the plant extract acts as the reducing agents by donating electrons to the metal ions, reducing them followed by stabilizing them in order to minimize the gathering of the nanoparticles.^{91,92} Furthermore, these phytochemicals also act as the capping agents by forming a layer on the surface of the nanoparticles, as evident from discussions made in a number of earlier literature.^{6,92–94,96}

The progression of nanoparticle synthesis was monitored visually from time to time (Figure 1B and C), and it was observed that the synthesis process of S4-GoNPs was very rapid, and there was an immediate change in the color of the solution from yellowish to dark purple after 5 min of addition of JLE to the reaction medium (Figure 1C). The entire process was prominent after 3 h of incubation, which was evident from the UV–VIS spectral analysis, which showed a steady peak at 538 nm (Figure 1B).

It is reported that, in aqueous solution, the spherical GoNPs displayed a spectrum of colors ranging from brown, orange, red, and purple as the core size increases from 1 to 100 nm, and usually display a size-relative absorption maximum between 500 and 550 nm.⁹⁹ Same phenomenon is observed in the current study (Figure 1C). For noble metal nanoparticles, light in the visible region of the electromagnetic spectrum couples to localized surface plasmon resonances, leading to intense destruction that causes colloidal interruptions of noble metal nanoparticles to display rich colors.^{100,101} Thus, in the case of the GoNPs, they show the complementary color of green or yellow, which is red or purple.¹⁰¹ The UV-VIS absorption spectroscopy measures the level at which the absorbing substance vitiate the electromagnetic radiations; further, it can also be used in the examination of variations in the absorption levels of

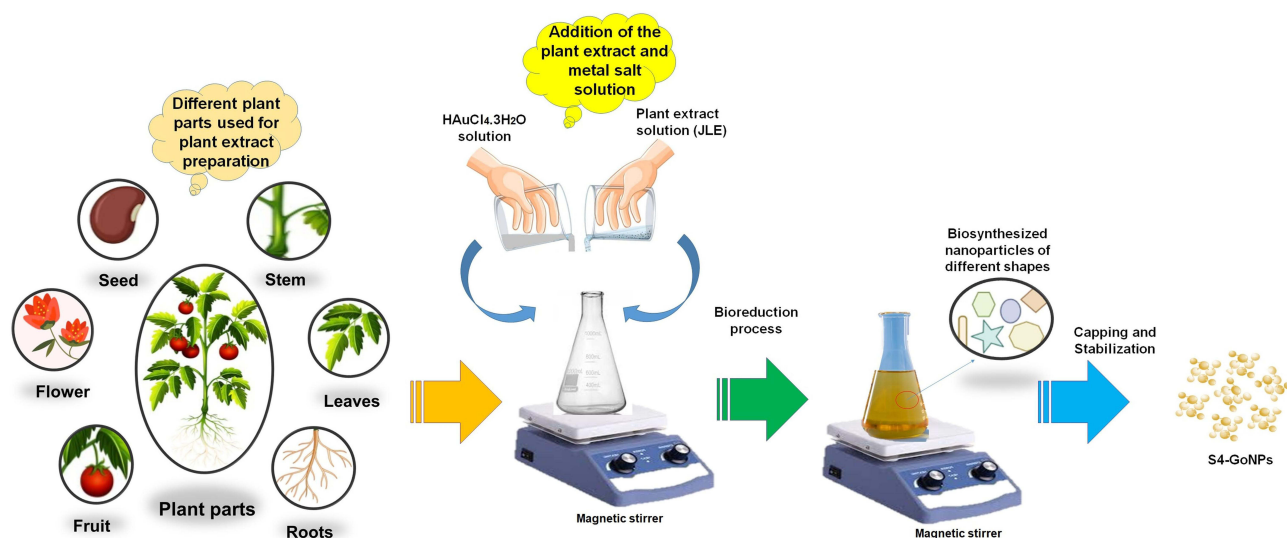


Figure 2 Schematic diagram showing the biosynthesis of gold nanoparticles using plant extracts.

individual compounds.²³ The phytochemical constituents of the Jamun leaf extract, such as polyphenols, flavonoids, tannins, carotenoids, and terpenoids, are involved in the bioreduction of Au³⁺ ions to Au⁰.¹⁹ Surface plasmon resonance is the oscillation of free electrons on the surface of a solid material, and it was found at 538 nm for S4-GoNPs (Figure 1B). Similar SPR in the range of 500–550 nm on gold nanoparticle synthesis using plant extracts has been reported earlier.¹⁰² Mie's theory for metal nanoparticles suggests the formation of SPR due to the free electrons and the single SPR band related to the creation of round nanoparticles, whereas the formation of two absorption peaks in UV–VIS scanning is related to the creation of irregular and anisotropic morphology.^{102–105} To confirm the stability, S4-GoNPs were maintained for 24 h, and the stable position of the SPR peak after 24 h confirmed the stable biosynthesis of the GoNPs (Figure 1B).

After confirming the synthesis of S4-GoNPs, they were subjected to several morphological, chemical, and physical characterizations. The morphology and elemental composition of the nanoparticles were determined using SEM-EDX analysis (Figure 3A and B). The SEM image demonstrates the uniform distribution of the spherical nanoparticles. However, the image shows agglomeration of the nanomaterials, which might be due to the use of a less advanced SEM machine for taking the images; however, when the said nanoparticles are visualized under the 2D AFM machine, clear and distinct spherical-shaped nanoparticles are observed that confirmed that the said nanoparticles are not aggregated. Moreover, due to the limited resolution of SEM, no clear differences in the size or shape of the obtained S4-GoNPs were observed. This result is similar to that obtained in previous publications.^{106,107} There are reports that green-synthesized nanoparticles are often agglomerated owing to the strong polarity and electrostatic attraction between nanoparticles.¹⁰⁸ It has been reported that sphere-shaped nanoparticles tend to agglomerate more easily because of the easy contact between adjacent particles, which might be the case in S4-GoNPs, which are spherical in nature.¹⁰⁹ Figure 3B shows the EDX spectra of S4-GoNPs. Typically, metallic nanoparticles show SPR absorption peaks in the range of 2–2.5 keV and which is also evident in our current study, the result of which showed an absorption peak at 2.2 keV (Figure 3B). This confirmed the successful manufacture of pure GoNPs. The presence of other peaks, such as carbon, nitrogen, and oxygen, could be due to the bioactive compounds present in JLE, which were used in the bioreduction synthesis of S4-GoNPs.¹¹⁰ Besides, another peak of silver (Ag) was seen in the EDX image, which is due to technical error from the machine, as its nonexistence was confirmed since its percent is 0% as evident from the associated table. Similar results have been previously published.^{102,106,111} The surface morphology of the S4-GoNPs, as shown by 2D and 3D AFM analyses with subnanometer resolution, showed morphology with clear and distinct spherical nanoparticles (Figure 3C and D). The 3D images revealed that the S4-GoNPs distribution was small. A direct scrutiny of the AFM images revealed that the size of the S4-GoNPs was in the range of 1–50 nm. Similar results have been previously reported for other gold nanomaterials.^{112–116}

XRD analysis depicts the crystalline structure of nanomaterials, owing to their ability to interact with the electrons of the inner shell of an atom.¹¹³ In the present study, the XRD spectra of S4-GoNPs were scanned from 10° to 90° (Figure 4A). The S4-GoNPs were in nanostructures, as demonstrated by Bragg's diffraction peaks at 2θ values of 38.20°, 44.37°, 64.77°, 77.56°, and 82.01°, matching the (111), (200), (220), (311), and (222) planes, which are identical to those of the normal gold metal Au⁰ (JCPDS card no. 04–0784).^{106,117} The diffraction peaks were related to the facets of the face-centered cubic (FCC) crystal lattice, and the widths of the corresponding planes were used to calculate the crystallite size.¹¹³ The average crystallite size of S4-GoNPs was calculated as 35.69 nm from the Scherrer equation,¹¹⁸ and a degree of crystallinity of 72.23% was calculated using the OriginPro 2024, version 10.1 software. Similarly, XRD diffraction peaks were also reported in another study on gold nanoparticle synthesis using *S. cumini* leaf extract.⁴² The intense diffraction peak at 38.20° confirmed that the preferred growth orientation of zero valent gold was fixed in (111) direction in a flat position on the planar surface (Figure 4A), and the current result attributes to the molecular-sized solids formed with an imitating 3D pattern of atoms or molecules with an equal distance between each part.^{119–121} Additionally, the reflections corresponding to (200), (220), (311), and (222) were feeble and extended, which demonstrates that the nanoparticles are of smaller size.^{121,122} This XRD pattern is typical of pure gold nanocrystals.¹¹⁹

The particle size distribution determined by DLS and the zeta potential analysis confirmed that the hydrodynamic diameter of S4-GoNPs was 120.5 nm with a Pdi of 0.152 and a zeta potential of –27.6 mV (Figure 4B and C). It is observed that the zeta potential data are a good indicator of degree of electrostatic interaction among the scattered particles and hence it is used for quantitative measurement of the charge-induced colloidal stability.^{123,124} It should be noted that the zeta potential was highly

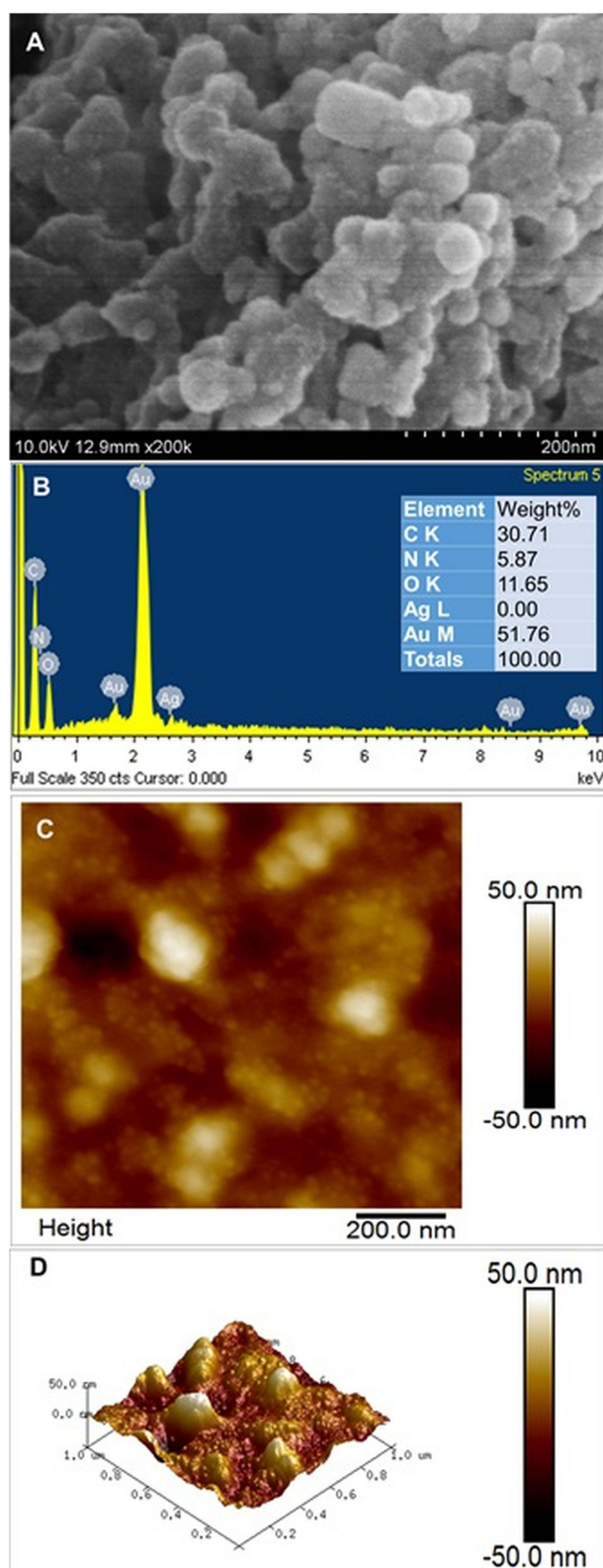


Figure 3 (A) SEM image of S4-GoNPs (inset: magnified view); (B) EDS spectra of S4-GoNPs; (C) 2D AFM image; (D) 3D AFM image.

negative, which indicated that the S4-GoNPs repel each other and are less likely to join together, resulting in the stability of the synthesized nanomaterial. Similar reports on the high zeta potential and their colloidal stability have also been reported in earlier published literatures.^{102,125–127} FTIR spectroscopy aids in molecular fingerprinting for the elucidation of organic

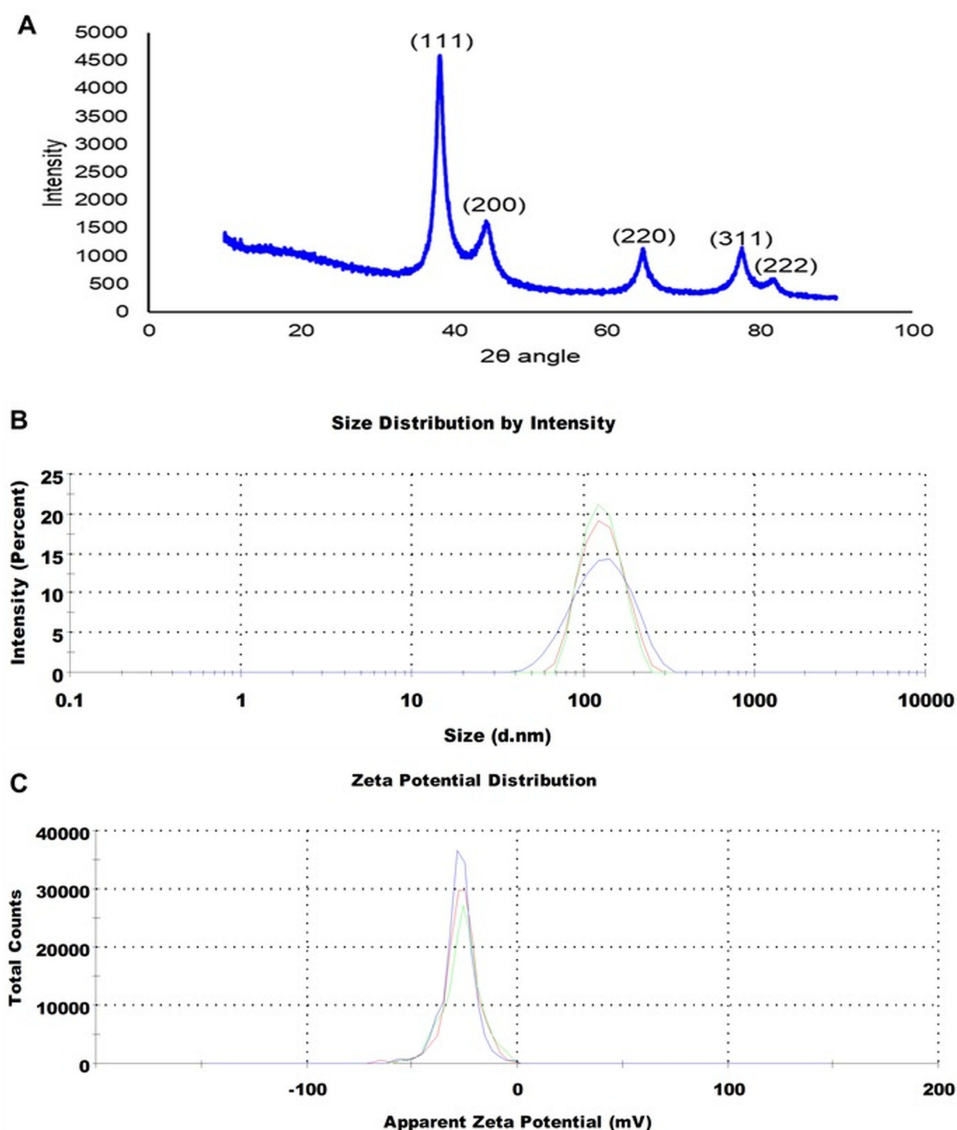


Figure 4 (A) XRD image of S4-GoNPs; (B) Particle size distribution and (C) Zeta potential of S4-GoNPs.

materials present in biological samples.¹¹³ FTIR analysis was performed to check for the presence of various types of functional groups present in the JLE, which may be responsible for the reduction, capping, and stabilization of S4-GoNPs. Around seven distinct peaks such as 3346.37 cm^{-1} representing O–H stretching, H-bond of alcohols; 1713.94 cm^{-1} representing C=O stretch of carbonyl group; 1603.52 cm^{-1} representing N–H bend of primary amines; 1441.05 cm^{-1} and 1363.91 cm^{-1} representing C–H bend of alkanes, methyl group; 1176.85 cm^{-1} represents C–O stretch of tertiary alcohol; and 1039.93 cm^{-1} representing C–N stretch of aliphatic amines was seen in case of the JLE (Figure 5A, Table 3). While in the S4-GoNPs, only six peaks such as 3332.91 cm^{-1} representing O–H stretching, H-bond of alcohols and phenols; 2110.71 cm^{-1} representing $\text{--C}\equiv\text{C--}$ stretch of alkynes; 1639.75 cm^{-1} representing C=O stretch of carbonyls (general); 664.84 cm^{-1} , 599.47 cm^{-1} , and 553.94 cm^{-1} representing C–Br stretch of alkyl halides with a halogen attached to it was seen (Figure 5A, Table 3).^{106,128,129} A similar report on the FT-IR spectra of jamun leaf extract was reported earlier, with three distinctive peaks at 3296.13 cm^{-1} , 2125.40 cm^{-1} , and 1635.85 cm^{-1} representing carboxylic acid, misc compounds, and amides stretch, respectively.¹³⁰ A deviation in the peak positions was observed in the S4-GoNPs from that of the JLE, which could be attributed to the utilization of the bioactive compounds from the JLE in the bioreduction, capping, and stabilization of the nanomaterials.¹³¹ In addition, it was proven that there was a weak intermolecular interaction and decrease in the

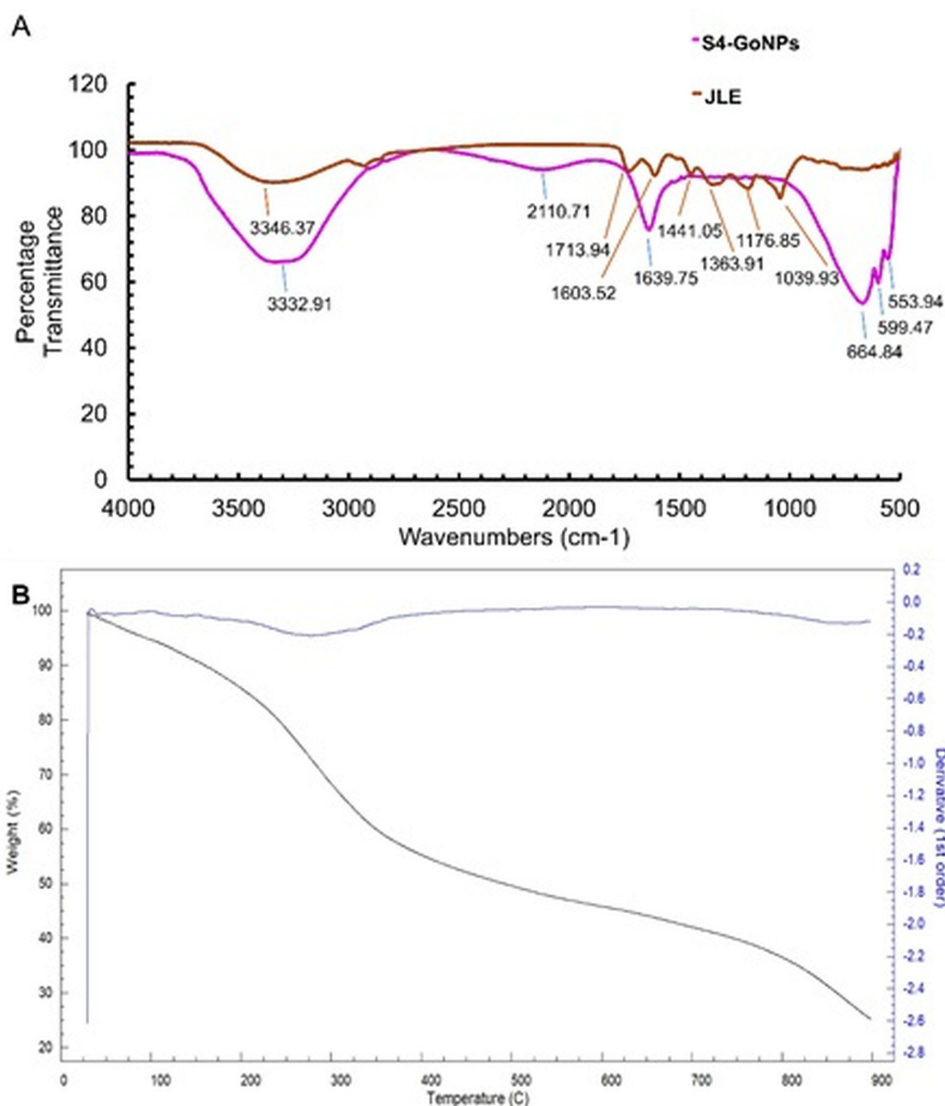


Figure 5 (A) FT-IR image of S4-GoNPs and JLE extract; (B) TGA image of S4-GoNPs.

mechanical properties between the S4-GoNPs and the JLE, which resulted in a slight decrease in the stretching vibrations to lower numbers in the case of the S4-GoNPs.¹³² The most significant change detected in the FTIR spectrum of S4-GoNPs was the shift of the 3346.37 cm⁻¹ wavenumber of JLE to a slightly lower wavenumber of 3332.91 cm⁻¹ in S4-GoNPs, representing the O–H stretching and H-bonding of alcohols and phenols. These shifting changes indicate that a new molecular interaction is probably exposed to hydrogen bonding, signifying that these groups were placed in a new chemical environment, as discussed in the earlier literature.¹³² All of these bands clearly indicate the presence of polyphenols, proteins, and flavonoids in JLE, which act as reductants for the GoNPs to be synthesized.^{106,110,113} The IR spectra denote the exact fingerprint of the components of a sample with the adsorption peaks corresponding to the vibration frequencies among different bonds of atoms comprising the specific compound. Because the different compounds are the exclusive groupings of various atoms, no two compounds can produce the same IR spectra; thus, the qualitative analysis of the components of the extracts can be properly identified by FT-IR analysis.¹³³

Finally, the decomposition effect of the S4-GoNPs was analyzed by the TGA analysis at high temperatures from 25° to 900°C (Figure 5B). The TGA graph depicts three-phase weight loss, starting from 29.83°C to 275.04°C (1st phase), accounting for 26.44% of weight loss, which might be due to the evaporation of thin-layer decomposition of water and other smaller molecules present on the outer surface of the nanoparticle (Figure 5B). The second phase of weight loss

Table 3 FTIR Analysis of JLE and S4-GoNPs

Extract Name	Peaks	Functional Groups Range	Vibrational Clusters
JLE	3346.37 cm^{-1}	Hydrogen bonded 3500–3200 cm^{-1}	O–H stretching, H-bond
	1713.94 cm^{-1}	The carbonyl stretch C=O of a carboxylic acid appears as an intense band from 1760–1690 cm^{-1} .	C=O stretch
	1603.52 cm^{-1}	From 1650–1580 cm^{-1} , amines	N–H bend of primary amines
	1441.05 cm^{-1}	From 1450–1375 cm^{-1} , alkenes, methyl group	C–H bend of alkanes
	1363.91 cm^{-1}	C–H rock, methyl from 1370–1350 cm^{-1}	C–H bend of alkanes
	1176.85 cm^{-1}	From 1205–1124 cm^{-1} , tertiary alcohol	C–O stretch of tertiary alcohol
	1039.93 cm^{-1}	CO–O–CO stretching anhydride	C–N stretch of aliphatic amines
S4-GoNPs	3332.91 cm^{-1}	Hydrogen bonded 3500–3200 cm^{-1}	O–H stretching, H-bond of alcohols and phenols
	2110.71 cm^{-1}	From 2260–2100 cm^{-1} , alkynes	–C≡C– stretch of alkynes
	1639.75 cm^{-1}	Carbonyl(C=O) stretching vibrations typically seen between 1800 and 1600 cm^{-1}	C=O stretch of carbonyls (general)
	664.84 cm^{-1}	C–X stretch 690–515 cm^{-1} of Alkyl halides (Alkyl halides are compounds that have a C–X bond, where X is a halogen: bromine, chlorine, fluorene, or iodine.)	C–X stretch of alkyl halides
	599.47 cm^{-1}		
	553.94 cm^{-1}		

from 275.04°C to 825.00°C accounting for a weight loss of 39.21% is due to the presence of organic matter and bioactive compounds from the JLE attached to the S4-GoNPs that could have aided in the bioreduction, capping, and the stabilization of the nanomaterials.^{134,135} This maximum weight loss during the second phase might be due to the increased number of intermolecular interactions for each S4-GoNP molecule with an increase in JLE concentration.¹³² The third phase of weight loss, from 825.00 to 900.00°C, corresponded to a 9.15% loss (Figure 5B). This might also be due to the decomposition of the residues and degradation of resistant aromatic compounds present in JLE.^{19,132,136,137} Based on the TGA results, the enhanced thermal strength of the S4-GoNPs can be attributed to the formation of hydrogen bonds between the GoNPs and JLE, as is evident from the FTIR analysis. Possibly, due to the changes witnessed in the crystallinity, from the second degradation temperature, the weight loss increased and achieved a maximum weight loss of 39.21% at 825.00°C which could be due to the interactions between the GoNPs and the JLE during the formation of S4-GoNPs.¹³²

After confirmation of the synthesis of S4-GoNPs, various types of biomedical applications, including antibacterial, antidiabetic, tyrosinase inhibition, antioxidant potential, and photocatalytic degradation of industrial dyes, were investigated. The antibacterial potential of the S4-GoNPs was evaluated by disc diffusion assay against seven foodborne pathogenic bacteria: *E. coli*, *E. faecium*, *A. hydrophila*, *S. Typhimurium*, *Pediococcus* sp., *B. cereus*, and *P. aeruginosa* (Tables 4 and 5, Figure 6).

The results depicted the potential effects of the S4-GoNPs against all tested pathogens, with the diameters of the zones of inhibition ranging between 11.02 – 14.12 mm at a concentration of 100 $\mu\text{g}/\text{disc}$ (Table 4, Figure 6). Among the tested pathogens, S4-GoNPs were more active against *E. faecium* (14.12 mm inhibition zone) and least active against *B. cereus* (11.02 mm inhibition zone). The results were compared with those of the positive reference standard antibiotic

Table 4 Antibacterial Effects of S4-GoNPs and Streptomycin Against the Pathogenic Bacteria

	<i>E. coli</i>	<i>E. faecium</i>	<i>A. hydrophila</i>	<i>S. Typhimurium</i>	<i>Pediococcus sp.</i>	<i>B. cereus</i>	<i>P. aeruginosa</i>
S4-GoNPs	11.93 ^g ±0.23	14.12 ^c ±0.36	11.34 ^{fg} ±0.84	12.89 ^d ±0.26	12.64 ^d ±0.09	11.02 ^{gh} ±0.26	11.77 ^{ef} ±0.11
Streptomycin	11.64 ^{ef} ±0.62	10.55 ^h ±0.19	15.99 ^b ±0.35	16.24 ^b ±0.08	–	15.84 ^b ±0.31	16.83 ^a ±0.28

Notes: *Data are presented as the mean diameter of inhibition zones (mm ± standard deviation). Numbers with different superscript letters are statistically significant at P<0.05.

Table 5 MIC and MBC of S4-GoNPs and Streptomycin Against Pathogenic Bacteria

Bacteria	S4-GoNPs		Streptomycin	
	MIC*	MBC*	MIC*	MBC*
<i>E. coli</i>	50*	100	5	10
<i>E. faecium</i>	50	100	10	>10
<i>A. hydrophila</i>	50	100	5	10
<i>S. Typhimurium</i>	50	100	5	10
<i>Pediococcus sp.</i>	50	100	–	–
<i>B. cereus</i>	>50	100	5	10
<i>P. aeruginosa</i>	50	100	5	10

Notes: *Values in µg/mL.

streptomycin, which showed inhibition zone diameters ranged from 10.55 – 16.24 mm at a concentration of 10 µg/disc (Table 4, Figure 6). Besides, streptomycin, other standard antibiotics were also tested; however, only the streptomycin that showed promising results against most of the pathogens are presented in the current study. However, streptomycin was ineffective against *B. cereus*. To determine the concentration of S4-GoNPs and streptomycin, bacterial growth was inhibited, or complete death of the bacteria was triggered, and the MIC and MBC values were checked against all pathogens, ranging between 50 and 100 µg/mL and 5 – >10 µg/mL, respectively (Table 5). The variation in the diameter of the zone of inhibition might be due to the morphological changes associated with each pathogenic bacterium, and it may be associated with the presence of hydroxyl groups in phenolic compounds and different chemical compounds present in JLE that acted as reducing and capping agents in the formulation of S4-GoNPs. These results confirmed that S4-GoNPs, because of their small size and configuration, are effective against a range of pathogens and could serve as an alternative solution against multidrug-resistant pathogens, where most of the standard antibiotics are ineffective. The probable mode of antibacterial action of the S4-GoNPs could be attributed to their smaller size, which might facilitate their easy penetration into the bacterial cell and consequential perforation of the cell membrane, leading to the release of cellular components outside, thereby causing immediate cellular lysis.^{46,138,139} In addition, other studies have reported that the presence of phenolic compounds could affect the phospholipid layers of the cell wall, resulting in membrane rupture,^{132,140} and this could also be the case in the current study, where the phenolic compounds present in JLE acting as capping agents in S4-GoNPs could be a reason for its antibacterial activity. In a study by Singh et al¹⁴¹ on the antioxidant and antimicrobial activity of the jambolan fruit polyphenols, the author has shown that the extract was active against a number of pathogens (*Staphylococcus aureus*, methicillin-resistant *S. aureus* [MRSA], *E. coli*, *Klebsiella pneumoniae*, and *Candida albicans*) with a zone of inhibition and minimum inhibitory concentration in the range from 14.3 – 23.0 mm and 0.5–2.5 mg/mL, respectively.¹⁴¹ However, in the current study, it was found that the diameter of the zone of inhibition exhibited by the S4-GoNPs ranged from 11.02 – 14.12 mm at a concentration of 100 µg/disc and MIC ranged between 50 and 100 µg/mL (Tables 4 and 5; Figure 6), which is much lower than previously reported. Similarly, in

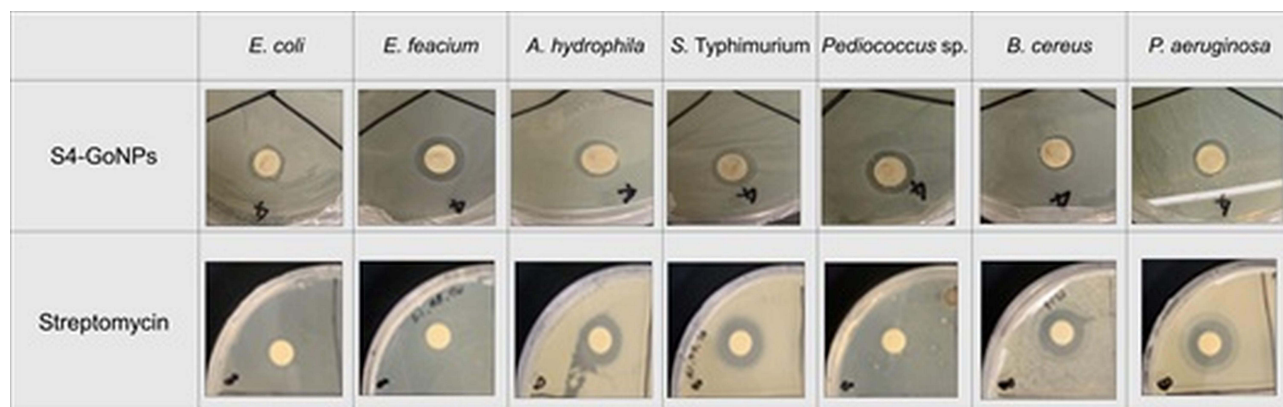


Figure 6 Antibacterial activity of S4-GoNPs and streptomycin against pathogenic bacteria.

another study, the authors reported the antibacterial activity of Jamun leaf extracts (in various nonpolar solvents such as petroleum ether, ethyl acetate, acetone, methanol, and ethanol), with maximum activity in petroleum ether and ethanolic solvents against *S. aureus* and *E. coli* (inhibition zone of 8–24 mm and MIC and MBC values varied from 1.56 25 mg/mL and 1.56 50 mg/mL).¹⁴² These results prove the effective potential of JLE, but they are much higher than those of S4-GoNPs in the current study (Tables 4 and 5; Figure 6). In an old report from 2007, the author has studied the antimicrobial activity of the Jamun leaf hydroalcoholic extracts against the pathogenic bacteria, namely, *Pseudomonas aeruginosa*, *Klebsiella pneumoniae*, and *S. aureus* 9.00–10.00 mm of inhibition diameter,¹⁴³ and the results are comparable to S4-GoNPs results. Diksha et al⁴² studied the antibacterial effects of AuNPs synthesized using the leaf extract of *S. cumini* against a number of pathogens, including *S. aureus*, *A. baumannii*, *E. coli*, *P. aeruginosa*, *E. faecalis*, *K. pneumoniae*, and *P. vulgaris* with MIC values ranging between 250 – 450 $\mu\text{g/mL}$.⁴² However, the current S4-GoNPs displayed a comparatively better MIC range of 50–100 $\mu\text{g/mL}$ (Tables 4 and 5; Figure 6), which proves the superior synthetic process and effective potential of S4-GoNPs. Other researchers have observed similar findings for plant extract-mediated GoNPs against a number of clinical and cultural bacterial strains and established considerable antibacterial activity.^{9,42,137,144,145} A further advantage of using nanoparticles in antibacterial treatment is that the bacteria are not able to mutate their genes in the nanoparticle-enabled treatment process.^{9,146}

α -Amylase and α -glucosidase enzyme assays were performed to study the antidiabetic potential of S4-GoNPs and the results showed promising outcomes as compared with the acarbose, taken as the reference-positive control (Figure 7A and B). The results demonstrated the potential antidiabetic effect of S4-GoNPs with approximately 28.97–40.67% of the α -amylase enzyme inhibition activity at three different concentrations (25–100 $\mu\text{g/mL}$) (Figure 7A). Meanwhile, acarbose as the positive control exhibited 48.46–61.62% inhibition activity at the same concentrations (Figure 7A). The effective concentration (IC_{50}) that inhibited 50% of α -amylase enzyme was found to be 120.94 $\mu\text{g/mL}$ for S4-GoNPs and 49.80 $\mu\text{g/mL}$ for acarbose (Table 6). Similarly, in the case of the α -glucosidase enzyme activity, the effect of S4-GoNPs ranged from 2.94% – 91.33%, with the maximum effect observed at the high concentrations of 50 $\mu\text{g/mL}$ (75.93%) and 100 $\mu\text{g/mL}$ (91.33%) (Figure 7B). Besides, acarbose, taken as a reference-positive control, displayed much lower α -glucosidase enzyme activity with 2.56–7.01% at the same concentrations. The effective concentration (IC_{50}) that inhibited 50% of α -glucosidase enzyme was found to be 43.83 $\mu\text{g/mL}$ for S4-GoNPs, whereas it was found as 771.08 $\mu\text{g/mL}$ for acarbose (Table 6). Linear regression analyses were performed using the SPSS statistical analysis software to determine the association between α -amylase and α -glucosidase, which showed a positive trend between the parameters (Figure 8A). The α -amylase enzyme is found in human saliva and is responsible for transforming complex starch molecules into their simpler form of glucose.¹⁴⁷ Therefore, inhibiting the effect of α -amylase in the body could be helpful in regulating carbohydrate metabolism in the body, subsequently reducing the amount of glucose absorbed.¹⁴⁷ Additionally, a key approach for the hindrance of a strident increase in blood sugar levels is to prevent the effect of the starch-blocking enzyme α -glucosidase.¹⁴⁷ Reports say that GoNPs have been shown to enhance the antioxidant system of the human body, thereby protecting the kidney cells from oxidative damages and reducing the risk of

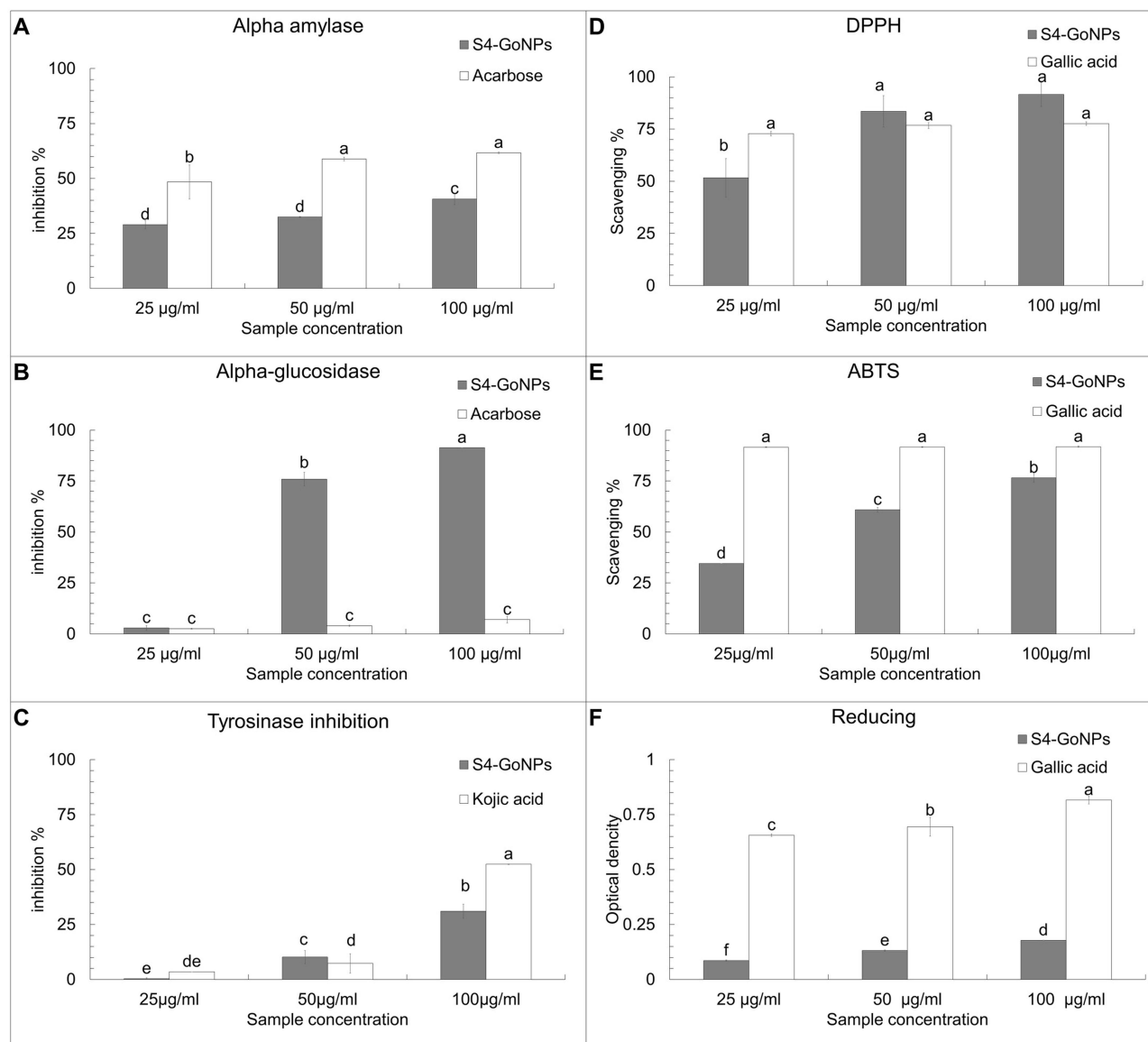


Figure 7 (A) α – amylase inhibition; (B) α – glucosidase; (C) tyrosinase inhibition; (D) DPPH scavenging; (E) ABTS scavenging and (F) Reducing power potential of S4-GoNPs. Each bar graph with different superscript letters defines statistical significance at $P < 0.05$.

progression of diabetic nephropathy.^{148,149} Ramachandran et al¹⁵⁰ concluded that wedelolactone mediated GoNPs were used successfully to regulate the Bcl-2 family proteins expression, and curtail the lipid peroxidation, in order to enhance the antioxidants and insulin secretions through the GLUT2 pathway in RIN-5F cell lines.¹⁵⁰ Plants contain a number of phytochemicals such as berberine, strychnine, asaronic acid, and apigenin, which have been used as plant-based diabetic drugs.¹⁵¹ Considering these, the GoNPs synthesis using plant extracts could be assumed to possess enhanced antidiabetic effects. In a study, Bakshi et al¹⁵² studied the antidiabetic potential of *S. cumini* leaf methanol extracts by both α -amylase and α -glucosidase enzyme inhibition activity and have found the inhibition activity with IC_{50} values of 48.34 and 30.15 $\mu\text{g/mL}$, respectively, for both the assays. In the current study, S4-GoNPs synthesized using aqueous JLE had IC_{50} values of 120.94 and 43.83 $\mu\text{g/mL}$ (Table 6) for both assays, which is comparable to the findings of Bakshi et al. Bakshi et al¹⁵² also studied the correlation between both assays and found a positive correlation between the parameters, which was corroborated by the results of our current study (Figure 8A). Furthermore, Poongunran et al¹⁵³ studied different leaf extracts of *S. cumini* (hexane, ethyl acetate, methanol, and water) to inhibit α -amylase activity, and found that the methanol and aqueous extracts performed better than the ethyl acetate extract at inhibiting α -amylase (IC_{50} of 61 and

Table 6 IC₅₀/ IC_{0.5} Values of Antidiabetic, Tyrosinase Inhibition, and Antioxidant Assays of S4-GoNPs

Assays	IC ₅₀ value (µg/mL)	
	S4-GoNPs	Reference Compounds
α-amylase	120.94	49.80 (acarbose)
α-glucosidase	43.83	771.08 (acarbose)
Tyrosinase inhibitory activity	203.57	95.38 (Kojic acid)
DPPH	36.25	38.07 (Gallic acid)
ABTS	47.51	31.79 (Gallic acid)
Reducing (IC _{0.5})	206.07	38.78 (Gallic acid)

48.3 µg/mL respectively) at a concentration of 200 µg/mL. These findings support our current results. In another study, Bhavi et al¹⁵⁴ have synthesized silver nanoparticles using the aqueous leaf extract of *S. cumini* and studied its α-amylase inhibition with an IC₅₀ value of 121.21 µg/mL for the nanoparticle and 193.29 µg/mL for the plant extract, which is comparatively higher than IC₅₀ value obtained for the S4-GoNPs (Table 6). Considering the above facts, it can be concluded that S4-GoNPs could serve as useful agents for antidiabetic treatment.

The tyrosinase enzyme inhibition potential of S4-GoNPs was investigated by using mushroom melanin-producing tyrosine enzyme and the result is shown in Figure 7C. The S4-GoNPs demonstrated a reasonable tyrosinase inhibition property at three different concentrations (25–100 µg/mL), with a maximum activity of 31.04% at 100 µg/mL, as

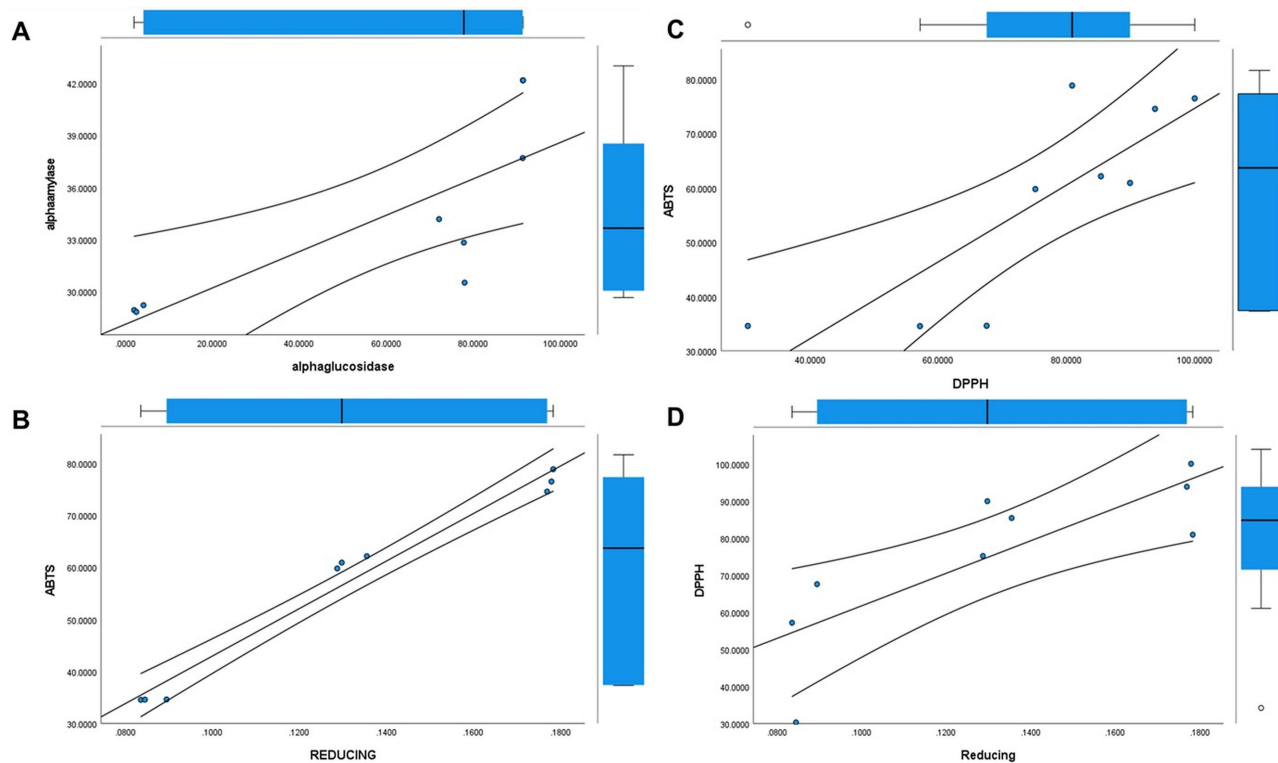


Figure 8 Regression analysis between (A) α – amylase and α – glucosidase enzyme assay; (B) ABTS and reducing assay; (C) ABTS and DPPH assay and (D) DPPH and Reducing power assay.

compared to kojic acid taken as the positive reference control with 52.3% inhibition activity at the same concentration of 100 $\mu\text{g/mL}$ (Figure 7C). The IC_{50} values of S4-GoNPs and the Kojic acid were found to be 203.57 and 95.38 $\mu\text{g/mL}$ (Table 6). In a study by Lima et al,¹⁵⁵ the tyrosinase inhibition activity of ethanolic extracts of *S. cumini* showed an IC_{50} of 219.52 $\mu\text{g/mL}$, which was higher than IC_{50} shown by S4-GoNPs (Table 6). Melanosomes are the location of melanin formation due to enzymatic reactions involving tyrosine as the substrate and tyrosinase.¹⁵⁶ Moreover, irregular melanin coloration in the body can be considered a severe aesthetic issue in humans, especially in middle-aged and elderly folks.^{156,157} It has been reported that there are many natural bioactive compounds that can inhibit tyrosinase enzymes or hinder or minimize melanin biosynthesis, which are considered useful in biological medicine for cosmetics.^{156–159} Alam et al¹⁶⁰ showed that the hydroxyl groups from phenolic compounds might hinder the enzymatic activity through the formation of hydrogen bonds with the tyrosinase enzyme active site, and some of the tyrosinase inhibitors act by binding their hydroxyl groups to the active site of the enzyme, subsequently leading to steric hindrance. The antioxidant activity could also play a vital role in tyrosinase inhibition activity.¹⁶⁰ The tyrosinase inhibitory mechanisms of the phenolic compounds showed that these phenolic compounds are able to act as copper chelators or compounds structurally mimicking the substrate of tyrosinase and can bind to a free enzyme of tyrosinase thereby preventing the substrate binding the enzyme active site.¹⁶¹ Hence, the S4-GoNPs synthesized using JLE rich in natural bioactive compounds such as phenols, acting as a tyrosinase inhibitor, hampering the formation of melanin, and thus could play a major role in skin hyperpigmentation by inhibiting the tyrosinase enzyme.

The antioxidant potential of the S4-GoNPs was investigated using DPPH, ABTS, and reducing power assays (Figure 7D–). The results of the DPPH scavenging assay showed a promising scavenging effect of the S4-GoNPs at 51.65%, 83.47%, and 91.56% at 25 $\mu\text{g/mL}$, 50 $\mu\text{g/mL}$, and 100 $\mu\text{g/mL}$, respectively (Figure 7D), compared to 72.79%, 76.70%, and 77.59% scavenging by the gallic acid used as the referred positive control at the same concentrations (Figure 7D). The IC_{50} values of S4-GoNPs and the Gallic acid for the DPPH assay were found to be 36.25 and 38.07 $\mu\text{g/mL}$, respectively (Table 6). Furthermore, the results of the ABTS scavenging assay showed 34.54, 60.91, and 76.59% effects, at 25 $\mu\text{g/mL}$, 50 $\mu\text{g/mL}$, and 100 $\mu\text{g/mL}$ by the S4-GoNPs (Figure 7E), respectively, compared to 91.63%, 91.67%, and 91.83% scavenging by the gallic acid taken as the reference-positive control at the same concentrations (Figure 7E). The IC_{50} values of S4-GoNPs and the Gallic acid for the ABTS assay were found to be 47.51 and 31.79 $\mu\text{g/mL}$, respectively (Table 6). In the reducing power assay, a positive increase in the OD value of the S4-GoNPs was observed (0.085, 0.131, and 0.177 OD) at 25 $\mu\text{g/mL}$, 50 $\mu\text{g/mL}$, and 100 $\mu\text{g/mL}$, respectively, to 0.656, 0.694, and 0.816 OD values compared to the reference-positive control, gallic acid (Figure 7F). These findings revealed that the antioxidant potential of S4-GoNPs increases at higher concentrations. The $\text{IC}_{0.5}$ values of S4-GoNPs and the Gallic acid for the reducing power assay were found to be 206.07 and 38.78 $\mu\text{g/mL}$, respectively (Table 6). The low IC_{50} values of S4-GoNPs demonstrated their strong antioxidant potential compared with the positive control compound. An optimistic trend was observed from the correlation study among the DPPH, ABTS, and reducing power assays with R^2 values of 0.826, 0.811, and 0.986, respectively, at 0.05 and 0.01 levels (Table 7), which signifies a strong positive correlation between the parameters (Table 7). To check the association between the antioxidant parameters, linear regression analyses were also performed, which showed a positive trend similar to that of the correlation analysis (Figure 8B–D).

Bakshi et al¹⁵² studied the antioxidant potential of *S. cumini* leaf methanol extracts by DPPH, ABTS, and superoxide scavenging assay and have found IC_{50} values of 42.34, 13.64, and 30.19 $\mu\text{g/mL}$, respectively, for the three assays. In the current investigation, S4-GoNPs synthesized using the aqueous JLE have the IC_{50} values of 36.25 and 47.51 $\mu\text{g/mL}$ for DPPH and ABTS activity, respectively (Table 6), which is comparable with the findings of Bakshi et al, since aqueous JLE extract was used in the current case for biosynthesis of S4-GoNPs. In addition, Bakshi et al¹⁵² reported a negative correlation (–0.20) between DPPH and ABTS assays, whereas we found a strong positive correlation (0.826) between the parameters (Table 7). In another study, the author evaluated the antioxidant (DPPH) activity of the methanolic extract of *S. cumini* leaves and reported an IC_{50} value of 125.39 $\mu\text{g/mL}$,¹⁶² which was much higher than the S4-GoNPs that showed an IC_{50} value of 36.25 $\mu\text{g/mL}$ (Table 6). The results showed that the S4-GoNPs synthesized using JLE had higher antioxidant potential than the aqueous leaf extracts of *S. cumini* (JLE in the current case). A study by Eshwarappa et al¹⁶³ concluded that the high content of total phenolics and flavonoids in the leaf gall extracts of *S. cumini* is responsible for its high antioxidant activity, which is also corroborated by the current study (Table 6, Figure 7). Phenolic antioxidants are

Table 7 Correlation Analysis of Antioxidant Parameters

	DPPH	ABTS	REDUCING
DPPH	1.000	0.826**	0.811**
ABTS		1.000	0.986**
REDUCING			1.000

Notes: ** Correlation is significant at the 0.01 level (2-tailed).

products of secondary metabolism in plants, and the antioxidant activity of these plants is primarily due to their redox potentials, which play a vital role in metal chelation, inhibition of lipoxygenase, and scavenging of free radicals.¹⁶⁴ Phenolic compounds are also known to be potential hydrogen donors, making them good antioxidant.¹⁶⁵ Oxidative stress can discharge free radicals, such as reactive oxygen species (ROS), networking with cytoplasmic enzymes or DNA that exaggerate or spread the difficulties of some precarious diseases, such as diabetic retinopathy, metastatic cancer, and neuropathy.¹⁶⁶ In addition, during biological nanoparticle functions, the ROS released could interfere with the Tumor Necrosis Factor receptors and decrease immune functions, resulting in the induction of cytotoxicity.¹⁶⁶ Hence, it is necessary to estimate the generation of free radicals or the shipping capacity of the nanoparticles while assessing their biomedical functions.¹⁶⁷ Antioxidant compounds play a major role in the safety machinery of the body against hazardous free radicals. There are reports that number of bioactive compounds such as 2(10)-Pinene; alfa-Copaene; alfa.-Muuroleone; alfa.-cadinene, etc, present in the JLE have been reported to possess antioxidant potentials.^{66,67,73,168–174} Thus, the positive effects of S4-GoNPs could be attributed to the utilization of JLE rich in these bioactive compounds, in the bio-reduction and stabilization of nanoparticles, which are rich in a number of bioactive phytochemicals.¹¹⁵ Similar studies on the antioxidant potential of nanoparticles have been recorded.^{25,166,175}

Following the biological potential study of S4-GoNPs, the photocatalytic degradation potential of the industrial cationic dye methylene blue was evaluated to highlight the potential of these nanoparticles to a broader extent (Figure 9A and B). The results revealed that with increased incubation time and exposure to light, the OD value intensity of the dye solution treated with S4-GoNPs was reduced at the absorption maximum peak point of 664 nm (specific to methylene blue dye) (Figure 9A). The OD values of the time-dependent degradation of the methylene blue dye solution were observed under UV light irradiation in the presence of S4-GoNPs. This suggests a discerning interface of cationic dyes with GoNPs and their removal from solution.¹⁷⁶ Similarly, a degradation percentage of 56.75% was attained after 5 h of light exposure (Figure 9B), which showed a positive increasing trend with an increase in the incubation period from 0 to 5 h (Figure 9B).

A number of studies on the photocatalytic degradation of methylene blue dye by different types of nanoparticles have been reported previously. In a study, Antony M et al¹⁷⁷ have reported the methylene blue dye degradation of nearly 80.57% by the gold nanoparticles coated with titanium dioxide nanotubes, after irradiation of sunlight for 240 min. In another study, Rodriguez Leon et al¹⁷⁸ showed that around 50% degradation of methylene blue dye was achieved by zeolite-Au nanocomposite in only 11 min in presence of sunlight. Similarly, Mondal et al¹⁷⁹ showed a degradation of 32.47% of methylene blue dye by the hydroxyapatite nanoparticles loaded with 0.055 wt% gold. Considering all the above discussions, it can be concluded that the effect of dye degradation depends on a number of factors such as the type of nanomaterials used, the process of light irradiation, and whether any types of combinations are added to the gold nanoparticles. Generally, nanoparticles are considered superlative photocatalysts because of their specific properties, such as stability, low cost, and high photoactive activity and during recent times, there have been more studies on nano adsorption and nano photocatalysis because of their extraordinary surface free energy and precise surface reactivity.^{180,181} The photocatalytic degradation of industrial dyes usually depends on the surface morphology, shape, and size of metallic nanoparticles.^{50,182} Moreover, some reports say that spherical nanoparticles demonstrate a superior photocatalytic degradation effect as compared to other forms of nanoparticles,^{50,183} which is also evident in the current study, where S4-GoNPs with a spherical shape exhibited promising photocatalytic degradation potential. A study by Li et al,¹⁸⁴ while investigating the photocatalytic degradation of sphere-like zinc ferrite nanostructures, has demonstrated

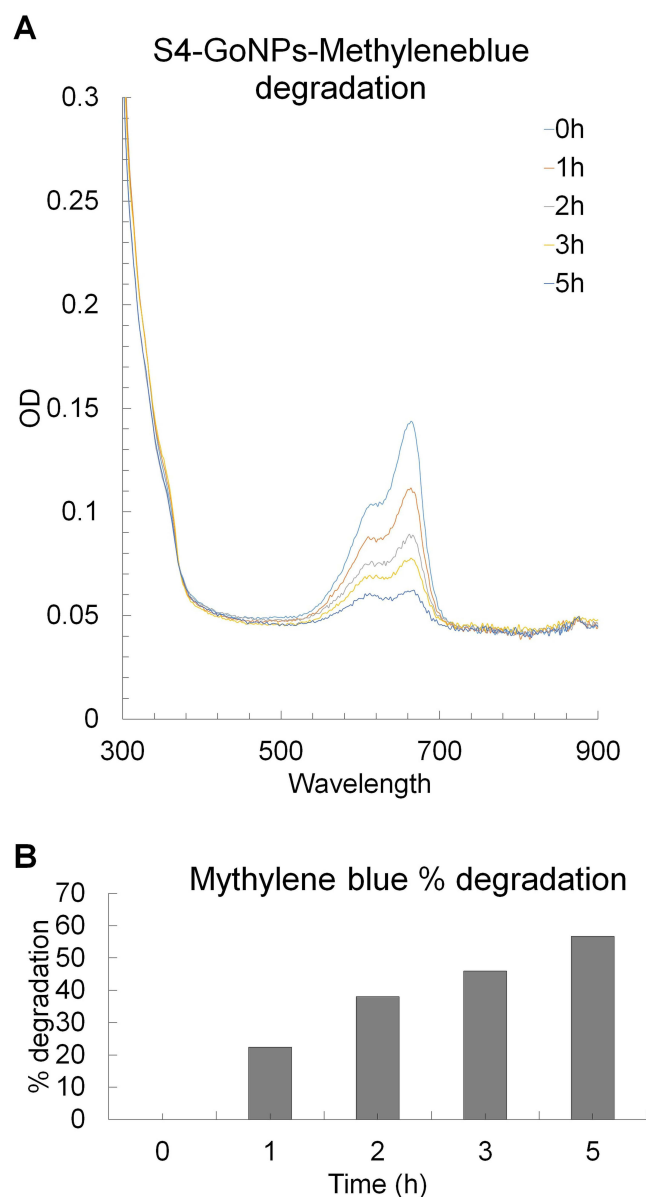


Figure 9 (A) Photocatalytic degradation of industrial toxic dye methylene blue by S4-GoNPs; **(B)** Degradation percentage.

that when only ZnFe_2O_4 nanoparticles were used as the catalyst, the photocatalytic degradation was 62.9%; however, when the same amount of ZnFe_2O_4 nanospheres was added as catalyst, its activity was increased to 100%. Further, the author clarified that since the photocatalytic reaction follows a pseudo-first-order reaction, and the kinetic constant over ZnFe_2O_4 nanospheres (0.6484 h^{-1}) was 2.93 times higher than that over the ZnFe_2O_4 nanoparticles (0.2211 h^{-1}), so the ZnFe_2O_4 nanospheres display much higher photocatalytic degradation activity than the ZnFe_2O_4 nanoparticles. Thus, in the current study, the enhanced photocatalytic degradation of S4-GoNPs could be attributed to the same principle of spherical shape exhibiting improved activity.

A possible mechanism of the photocatalytic reaction upon exposure to UV light comprises the manufacture of electron-hole pairs and splitting of conduction band electrons and valence band holes on the surface of S4-GoNPs.^{185,186} A schematic diagram showing the possible mode of action of the methylene blue dye is presented in Figure 10. It is postulated that increasing the charge separation and extending the absorption spectrum of light have resulted in the localized SPR effect that permitted the photocatalytic effect of the nanoparticles thereby degrading the dye.^{176,187,188}

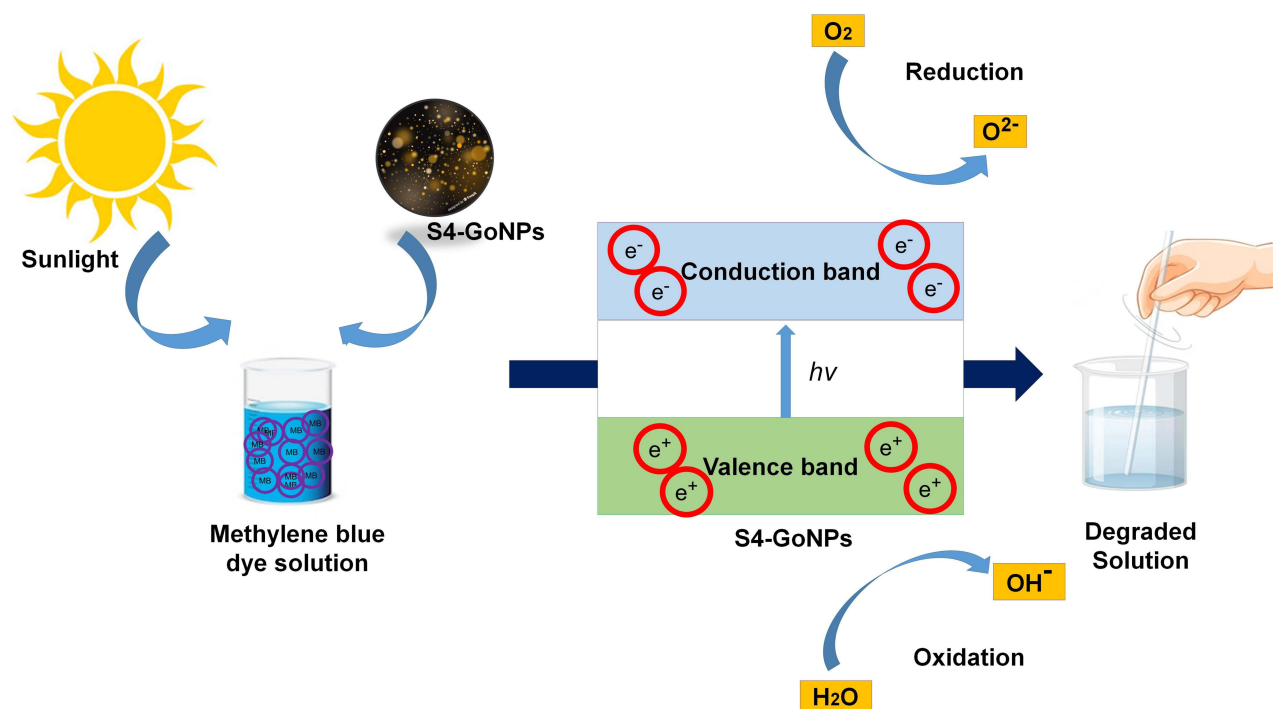


Figure 10 A possible mode of action of methylene blue dye degradation by the S4-AuNPs.

Methylene blue is a phenothiazine derivative used for dyeing textiles and is a highly toxic and carcinogenic dye.¹⁸⁹ In a study by Riaz et al,¹⁹⁰ the authors investigated the photocatalytic degradation of Congo red and methylene blue dyes using nickel oxide nanoparticles synthesized by the leaf extract of *S. cumini* and showed that the nanoparticles demonstrated high removal efficiency, which was also observed in our current investigation. Various conventional methods, such as ozonation and adsorption, are typically used for the removal of toxic dyes from wastewater; however, it is impossible to completely eliminate them from wastewater.^{191,192} Thus, metallic GoNPs can serve as an alternative tool for dye degradation. There are many reports on the photocatalytic degradation of industrial toxic dyes using plant extract-mediated biosynthesized nanoparticles,^{176,193,194} and the current study also supports these reports.

Conclusion

Green synthesis of biomediated metal nanoparticles has achieved widespread responsiveness over other conventional methods like chemical and physical methods because of their environment friendly, non-toxic, and cost-effective nature, together with enhanced biocompatibility. Further, the chemical and physical methods utilize large amounts of energy, release toxic and harmful chemicals, and use complex equipment and synthesis conditions. Besides the physical method of nanoparticle synthesis includes aerosols, ultraviolet radiation and thermal decompositions that require very high temperature and pressure. However, this is not the case, in the green synthesis method and it uses a one-pot synthesis process at room temperature and pressure condition and releasing almost no toxic byproducts and thus making it a more adaptable and environmentally friendly method of nanoparticle synthesis. They have also proven to be effective in numerous biological and environmental applications. This study presents an eco-friendly approach for the biomediated green synthesis of S4-GoNPs using jamun leaf aqueous extract (JLE) containing sufficient amounts of phytochemicals such as phenols, tannins, flavonoids, and cardiac glycosides. The S4-GoNPs were characterized using diverse analytical techniques to reveal their morphology, surface behavior, functionalities, and crystallinities. The SPR of the S4-GoNPs was found to be 538 nm with the absorption peak at 2.2 keV, and the average particle size by the particle size analyzer was determined as 120.5 nm with Pdi 0.152 and the zeta potential of -27.6 mV. The S4-GoNPs displayed promising biomedical applications, such as antibacterial effects (with a diameter of zones of inhibition ranging between 11.02 – 14.12 mm), significant antidiabetic properties (40.67% of α -amylase

and 91.33% of α -glucosidase enzyme inhibition), positive tyrosinase inhibition and antioxidant effects. In addition, S4-GoNPs also showed potential for photo-mediated toxic industrial dye degradation. The synthesized S4-GoNPs demonstrated improved biological activities, which could be attributed to the synergetic addition of biologically active adsorbed phytochemicals from the JLE, which operates as a reducing, coating, and alleviating agent in the green synthesis method. Its antibacterial, antioxidant, and tyrosinase inhibition potential could be beneficial for the food and cosmetics industries for formulating sunscreen lotions, anti-aging creams, and a number of similar uses. In addition, these nanoparticles could also be explored for antibacterial finishing of medical devices and instruments owing to their positive antibacterial potential. Metallic GoNPs for dye degradation can be utilized in the manufacture of industrial devices for toxic dye degradation. The S4-GoNPs, being synthesized by the green technology method, offer advantages over other types of nanoparticles synthesized using the chemical and physical methods and are very low cost and non-toxic, making them more suitable and have the potential for wider implementation in numerous biomedical research and environmental remediation. Further research on developing cosmetic formulations and drugs related to the displayed biological activities, exploring the scalability of the synthesis process, long-term stability of the nanoparticles, or potential regulatory considerations for their use in consumer products can be explored in future research.

Data Sharing Statement

All data related to this manuscript are available in the manuscript as Tables and Figures, and in the [supplementary data file](#).

Acknowledgments

All authors are grateful to Dongguk University, Republic of Korea, for their support. We are grateful to all whoever helped in the current research. We acknowledge the freepik.com website for using their images in preparing our schematic diagrams.

Disclosure

The authors declare that no conflicts of interest exist with this paper.

References

1. Ahamed M, AlSalhi MS, Siddiqui M. Silver nanoparticle applications and human health. *Clin Chim Acta*. 2010;411(23–24):1841–1848. doi:10.1016/j.cca.2010.08.016
2. Randhwan R, Patil D, Rajurkar S, et al. A novel green synthesis of *Syzygium cumini* leaves extract coated silver nanoparticles. *Chem Sci Rev Lett*. 2022;11(44):388–391.
3. Kaval U, Hoşgören H. Biosynthesis, characterization, and biomedical applications of gold nanoparticles with *Cucurbita moschata* Duchesne Ex Poiré peel aqueous extracts. *Molecules*. 2024;29(5):923. doi:10.3390/molecules29050923
4. Vijayaraghavan K, Ashokkumar T. Plant-mediated biosynthesis of metallic nanoparticles: a review of literature, factors affecting synthesis, characterization techniques and applications. *J Environ Chem Engineer*. 2017;5(5):4866–4883. doi:10.1016/j.jece.2017.09.026
5. Kessler R. *Engineered Nanoparticles in Consumer Products: Understanding a New Ingredient*. National Institute of Environmental Health Sciences; 2011.
6. Singh H, Desimone MF, Pandya S, et al. Revisiting the green synthesis of nanoparticles: uncovering influences of plant extracts as reducing agents for enhanced synthesis efficiency and its biomedical applications. *Int J Nanomed*. 2023;18:4727–4750. doi:10.2147/IJN.S419369
7. Vance ME, Kuiken T, Vejerano EP, et al. Nanotechnology in the real world: redeveloping the nanomaterial consumer products inventory. *Beilstein J Nanotechnol*. 2015;6(1):1769–1780. doi:10.3762/bjnano.6.181
8. Prasad R, Swamy VS. Antibacterial activity of silver nanoparticles synthesized by bark extract of *Syzygium cumini*. *J Nanopart Res*. 2013;2013:1–6. doi:10.1155/2013/431218
9. Ahmad S, Ahmad S, Xu Q, et al. Green synthesis of gold and silver nanoparticles using crude extract of *Aconitum violaceum* and evaluation of their antibacterial, antioxidant and photocatalytic activities. *Frontier Bioengineer Biotechnol*. 2023;11:1320739.
10. Manojkumar U, Kaliannan D, Srinivasan V, et al. Green synthesis of zinc oxide nanoparticles using *Brassica oleracea* var. botrytis leaf extract: photocatalytic, antimicrobial and larvicidal activity. *Chemosphere*. 2023;323:138263. doi:10.1016/j.chemosphere.2023.138263
11. Liu M, Xue X, Karmakar B, et al. Sonochemical synthesis of gold nanoparticles mediated by potato starch: its performance in the treatment of esophageal cancer. *Open Chem*. 2024;22(1):20230193. doi:10.1515/chem-2023-0193
12. Chokriwal A, Sharma MM, Singh A. Biological synthesis of nanoparticles using bacteria and their applications. *Am J PharmTech Res*. 2014;4(6):38–61.
13. Gur T, Meydan I, Seckin H, Bekmezci M, Sen F. Green synthesis, characterization and bioactivity of biogenic zinc oxide nanoparticles. *Environ Res*. 2022;204:111897. doi:10.1016/j.envres.2021.111897
14. Muddapur UM, Alshehri S, Ghoneim MM, et al. Plant-based synthesis of gold nanoparticles and theranostic applications: a review. *Molecules*. 2022;27(4):1391. doi:10.3390/molecules27041391

15. Chandraker SK, Lal M, Khanam F, Dhruve P, Singh RP, Shukla R. Therapeutic potential of biogenic and optimized silver nanoparticles using *Rubia cordifolia* L. leaf extract. *Sci Rep.* 2022;12(1):8831. doi:10.1038/s41598-022-12878-y
16. Bordiwala RV. Green synthesis and applications of metal nanoparticles.-A review article. *Results Chem.* 2023;5:100832. doi:10.1016/j.rechem.2023.100832
17. Karthik K, Raghu A, Reddy KR, et al. Green synthesis of Cu-doped ZnO nanoparticles and its application for the photocatalytic degradation of hazardous organic pollutants. *Chemosphere.* 2022;287:132081. doi:10.1016/j.chemosphere.2021.132081
18. Mustapha T, Misni N, Ithnin NR, Daskum AM, Unyah NZ. A review on plants and microorganisms mediated synthesis of silver nanoparticles, role of plants metabolites and applications. *Int J Environ Res Public Health.* 2022;19(2):674. doi:10.3390/ijerph19020674
19. Soto KM, López-Romero JM, Mendoza S, et al. Rapid and facile synthesis of gold nanoparticles with two Mexican medicinal plants and a comparison with traditional chemical synthesis. *Mater Chem Phys.* 2023;295:127109. doi:10.1016/j.matchemphys.2022.127109
20. Liao WC, Liao CS, Lin Y-C, Lien C-Y. Characterization of gold nanoparticles synthesized with *Zingiber zerumbet* extracts. *J Chem.* 2024;2024:1-8. doi:10.1155/2024/1358495
21. Lazarides A, Kelly KL, Jensen T, Schatz G. Optical properties of metal nanoparticles and nanoparticle aggregates important in biosensors. *J Mol Str.* 2000;529(1-3):59-63. doi:10.1016/S0166-1280(00)00532-7
22. Al-Radadi NS, Al-Bishri WM, Salem NA, ElShebiny SA. Plant-mediated green synthesis of gold nanoparticles using an aqueous extract of *Passiflora ligularis*, optimization, characterizations, and their neuroprotective effect on propionic acid-induced autism in Wistar rats. *Saudi Pharma J.* 2024;32(2):101921. doi:10.1016/j.jsps.2023.101921
23. Jabir MS, Abood NA, Jawad MH, et al. Gold nanoparticles loaded TNF- α and CALNN peptide as a drug delivery system and promising therapeutic agent for breast cancer cells. *Material Technol.* 2022;37(14):3152-3166. doi:10.1080/10667857.2022.2133073
24. Al-Radadi NS. Facile one-step green synthesis of gold nanoparticles (AuNp) using licorice root extract: antimicrobial and anticancer study against HepG2 cell line. *Arab J Chem.* 2021;14(2):102956. doi:10.1016/j.arabjc.2020.102956
25. Lopez-Chaves C, Soto-Alvaredo J, Montes-Bayon M, Bettmer J, Llopis J, Sanchez-Gonzalez C. Gold nanoparticles: distribution, bioaccumulation and toxicity. In vitro and in vivo studies. *Nanomed Nanotechnol Biol Med.* 2018;14(1):1-12. doi:10.1016/j.nano.2017.08.011
26. Mary SJ, Veeravarmal V, Thankappan P, Arumugam P, Augustine PI, Franklin R. Anti-cancer effects of green synthesized gold nanoparticles using leaf extract of *Annona muricata*. L against squamous cell carcinoma cell line 15 through apoptotic pathway. *Dent Res J.* 2024;21(1):14. doi:10.4103/drj.drj_521_23
27. Fakhri MA, Salim ET, Sulaiman GM, et al. Gold nanowires based on photonic crystal fiber by laser ablation in liquid to improve colon biosensor. *Plasmonics.* 2023;18(6):2447-2463. doi:10.1007/s11468-023-01961-3
28. Al Rugaie O, Jabir MS, Mohammed MK, et al. Modification of SWCNTs with hybrid materials ZnO-Ag and ZnO-Au for enhancing bactericidal activity of phagocytic cells against *Escherichia coli* through NOX2 pathway. *Sci Rep.* 2022;12(1):17203. doi:10.1038/s41598-022-22193-1
29. Jawad KH, Jamagh FK, Sulaiman GM, et al. Antibacterial and antibiofilm activities of amikacin-conjugated gold nanoparticles: a promising formulation for contact lens preservation. *Inorgan Chem Commun.* 2024;162:112286. doi:10.1016/j.inoche.2024.112286
30. Ayyanar M, Subash-Babu P. *Syzygium cumini* (L.) Skeels: a review of its phytochemical constituents and traditional uses. *Asian Pac J Trop Biomed.* 2012;2(3):240-246. doi:10.1016/S2221-1691(12)60050-1
31. Bernardo W, Boriollo MFG, Tonon CC, et al. Biosynthesis of silver nanoparticles from *Syzygium cumini* leaves and their potential effects on odontogenic pathogens and biofilms. *Frontier Microbiol.* 2022;13:995521. doi:10.3389/fmicb.2022.995521
32. Jain SK. *Dictionary of Indian Folk Medicine and Ethnobotany*. New Delhi, India: Deep publications; 1991.
33. Shrikant Baslingappa S, Nayan Singh JT, Meghatai MP, Parag MH. Jamun (*Syzygium cumini* (L.)): a review of its food and medicinal uses. *Food Nutri Sci.* 2012;2012.
34. Kumari N, Kumar M, Chaudhary N, et al. Exploring the chemical and biological potential of Jamun (*Syzygium cumini* (L.) Skeels) leaves: a comprehensive review. *Chem Biodivers.* 2023;20(9):e202300479. doi:10.1002/cbdv.202300479
35. Shidiki A, Vyas A. Molecular docking and pharmacokinetic prediction of phytochemicals from *Syzygium cumini* in interaction with penicillin-binding protein 2a and erythromycin ribosomal methylase of *Staphylococcus aureus*. *Biotechnologia.* 2022;103(1):5-18. doi:10.5114/bta.2022.113910
36. Kirtikar K, Basu B. *Indian Medicinal Plants*. Vols. I-IV. Dehradun: International Book Distributors; 1987.
37. Ahmad N, Nawab M, Kazmi MH. Medicinal potential of jamun (*Syzygium cumini* Linn): a review. *J Drug Del Therapeut.* 2019;9(5):175-180. doi:10.22270/jddt.v9i5.3568
38. Ayyanar M, Subash-Babu P, Ignacimuthu S. *Syzygium cumini* (L.) Skeels: a novel therapeutic agent for diabetes: folk medicinal and pharmacological evidences. *Complement Thera Med.* 2013;21(3):232-243. doi:10.1016/j.ctim.2013.03.004
39. Prasad M, Venugopal SP, Alagarsamy V, Sridevi C. The preliminary phytochemical analysis and oral acute toxicity study of stem bark of *Syzygium cumini*. *Int J Pharm Pharm Sci.* 2016;8(1):209-213.
40. Rajkumar G, Jayasinghe MR, Vinotha S. Comparative analytical study of phytochemicals in selected antidiabetic medicinal plant seeds in Sri Lanka. *Pharma Sci Res.* 2021;8(3):145-155.
41. Painuli R, Joshi P, Kumar D. Cost-effective synthesis of bifunctional silver nanoparticles for simultaneous colorimetric detection of Al(III) and disinfection. *Sensor Actuator B.* 2018;272:79-90. doi:10.1016/j.snb.2018.05.131
42. Diksha D, Gupta SK, Gupta P, Banerjee UC, Kalita D. Antibacterial potential of gold nanoparticles synthesized from leaf extract of *Syzygium cumini* against multidrug-resistant urinary tract pathogens. *Cureus.* 2023;15(2):e34830. doi:10.7759/cureus.34830
43. Ravikumar V, Gopal V, Sudha T. Analysis of phytochemical constituents of stem bark extracts of *Zanthoxylum Tetraspermum* Wight & Arn. *Res J Pharma Biol Chem Sci.* 2012;3(4):391-402.
44. Sofowora A. *Medicinal Plants and Medicine in Africa*. Ibadan Nigeria: John Wiley Spectrum; 1993:281-285.
45. Das G, Seo S, Yang JJ, Nguyen LTH, Shin HS, Patra JK. Synthesis of biogenic gold nanoparticles by using sericin protein from *Bombyx mori* silk cocoon and investigation of its wound healing, antioxidant, and antibacterial potentials. *Int J Nanomed.* 2023;18:17-34. doi:10.2147/IJN.S378806
46. Patra JK, Baek K-H. Novel green synthesis of gold nanoparticles using *Citrullus lanatus* rind and investigation of proteasome inhibitory activity, antibacterial, and antioxidant potential. *Int J Nanomed.* 2015;10:7253.

47. Ali H, Houghton P, Soumyanath A. α -Amylase inhibitory activity of some Malaysian plants used to treat diabetes; with particular reference to *Phyllanthus amarus*. *J Ethnopharmacol*. 2006;107(3):449–455. doi:10.1016/j.jep.2006.04.004
48. Gowri PM, Tiwari AK, Ali AZ, Rao JM. Inhibition of α -glucosidase and amylase by bartogenic acid isolated from *Barringtonia racemosa* Roxb. seeds. *Phytother Res*. 2007;21(8):796–799. doi:10.1002/ptr.2176
49. Patra JK, Das G, Shin H-S. Facile green biosynthesis of silver nanoparticles using *Pisum sativum* L. outer peel aqueous extract and its antidiabetic, cytotoxicity, antioxidant, and antibacterial activity. *Int J Nanomed*. 2019;14:6679–6690. doi:10.2147/IJN.S212614
50. Selvam K, Albasher G, Alamri O, et al. Enhanced photocatalytic activity of novel *Canthium coromandelicum* leaves based copper oxide nanoparticles for the degradation of textile dyes. *Environ Res*. 2022;211:113046. doi:10.1016/j.envres.2022.113046
51. Yugandhar P, Vasavi T, Shanmugam B, Devi PUM, Reddy KS, Savithamma N. Biofabrication, characterization and evaluation of photocatalytic dye degradation efficiency of *Syzygium alternifolium* leaf extract mediated copper oxide nanoparticles. *Mater Res Expr*. 2019;6(6):065034. doi:10.1088/2053-1591/ab0db9
52. Tambe BD, Pedhekar P, Harshali P. Phytochemical screening and antibacterial activity of *Syzygium cumini* (L.) (Myrtaceae) leaves extracts. *Asian J Pharma Res Develop*. 2021;9(5):50–54. doi:10.22270/ajprd.v9i5.1023
53. Kumar A, Kalakoti M. Phytochemical and antioxidant screening of leaf extract of *Syzygium cumini*. *Int J Adv Res*. 2015;3(1):371–378.
54. Mubassara S, Biswas KK, Hasan MM, Hossain MI, Paul S. In vitro phytochemical, antibacterial and antioxidant analyses in different plant parts of *Syzygium cumini*. *Int J Pharmacog Phytochem Res*. 2015;7(1):150–155.
55. Jagetia GC. Phytochemical composition and pleotropic pharmacological properties of jamun, *Syzygium cumini* skeels. *J Explor Res Pharmacol*. 2017;2(2):54–66. doi:10.14218/JERP.2016.00038
56. Qamar M, Akhtar S, Ismail T, et al. Phytochemical profile, biological properties, and food applications of the medicinal plant *Syzygium cumini*. *Foods*. 2022;11(3):378.
57. Bari T, Saeed S, Tayyab M, Anjum AA, Mehmood T. GC-MS bioactives profiling, antibacterial and cytotoxic potential of Jamun (*Syzygium cumini* L.) extracts against food-Borne pathogen *Salmonella enteritidis*. *Pharma Chem J*. 2024;1–7.
58. Prabhakaran S, Gothandam K, Sivashanmugam K. Phytochemical and antimicrobial properties of *Syzygium cumini* an ethanomedicinal plant of Javadhu hills. *Res Pharma*. 2011;1(1):22–32.
59. Franco RR, Zabisky LFR, de Lima Júnior JP, et al. Antidiabetic effects of *Syzygium cumini* leaves: a non-hemolytic plant with potential against process of oxidation, glycation, inflammation and digestive enzymes catalysis. *J Ethnopharmacol*. 2020;261:113132. doi:10.1016/j.jep.2020.113132
60. Scalbert A, Johnson IT, Saltmarsh M. Polyphenols: antioxidants and beyond. *Am J Clin Nutr*. 2005;81(1):215S–217S. doi:10.1093/ajcn/81.1.215S
61. Mahmoud II, Marzouk MSA, Moharram FA, El-Gindi MR, Hassan AMK. Acylated flavonol glycosides from *Eugenia jambolana* leaves. *Phytochem*. 2001;58(8):1239–1244. doi:10.1016/S0031-9422(01)00365-X
62. Shafi PM, Rosamma MK, Jamil K, Reddy PS. Antibacterial activity of *Syzygium cumini* and *Syzygium travancoricum* leaf essential oils. *Fitoterapia*. 2002;73(5):414–416. doi:10.1016/S0367-326X(02)00131-4
63. Elansary HO, Salem MZ, Ashmawy NA, Yacout MM. Chemical composition, antibacterial and antioxidant activities of leaves essential oils from *Syzygium cumini* L. *Cupressus sempervirens* L. and *Lantana camara* L. from Egypt. *J Agri Sci*. 2012;4(10):144.
64. Vivek J, Sagar M, Keyuri B, et al. Chromatographic profiling of *Syzygium cumini* leaves using high-performance thin layer chromatography and gas chromatography-mass spectrometry techniques. *Malay J Anal Sci*. 2021;25(5):808–820.
65. Dan S, Rajwar S, Mandal M, Bhatnagar T. Quantitative analysis of phytochemical constituents and antioxidant assay of *Syzygium cumini* leaf. *Der Pharmacia Lettre*. 2022;14(5):16–25.
66. Salehi B, Upadhyay S, Erdogan Orhan I, et al. Therapeutic Potential of α - and β -Pinene: a Miracle Gift of Nature. *Biomolecules*. 2019;9(11):738. doi:10.3390/biom9110738
67. da Silva Rivas AC, Lopes PM, de Azevedo Barros MM, Costa Machado DC, Alviano CS, Alviano DS. Biological activities of α -pinene and β -pinene enantiomers. *Molecules*. 2012;17(6):6305–6316. doi:10.3390/molecules17066305
68. Dhalani J, Dubal G, Patel A, Nariya P, Gondaliy M, Purohit D. Isolation and identification of nonpolar chemical entity from *Leptadenia Reticulata* aerial parts. *Asian J Pharma Clin Res*. 2019;12:226–229. doi:10.22159/ajpcr.2019.v12i2.28683
69. Kim D-S, Lee H-J, Jeon Y-D, et al. Alpha-pinene exhibits anti-inflammatory activity through the suppression of MAPKs and the NF- κ B pathway in mouse peritoneal macrophages. *Ame J Chinese Med*. 2015;43(4):731–742. doi:10.1142/S0192415X15500457
70. Him A, Ozbek H, Turel I, Oner AC. Antinociceptive activity of alpha-pinene and fenchone. *Pharmacologyonline*. 2008;3(7):363–369.
71. Lull C, Gil-Ortiz R, Cantin Á. A chemical approach to obtaining α -copaene from clove oil and its application in the control of the medfly. *Appl Sci*. 2023;13(9):5622. doi:10.3390/app13095622
72. Clarke S. Chapter 7 - Composition of essential oils and other materials. In: Clarke S, editor. *Essential Chemistry for Aromatherapy*. 2nd ed. Edinburgh: Churchill Livingstone; 2008:123–229.
73. Türkez H, Celik K, Toğar B. Effects of copaene, a tricyclic sesquiterpene, on human lymphocytes cells in vitro. *Cytotechnol*. 2014;66(4):597–603. doi:10.1007/s10616-013-9611-1
74. Schmeda-Hirschmann G, Theoduloz C. *Fabiana imbricata* Ruiz et Pav. (Solanaceae), a review of an important Patagonian medicinal plant. *J Ethnopharmacol*. 2019;228:26–39. doi:10.1016/j.jep.2018.09.020
75. González AM, Tracanna MI, Amani SM, et al. Chemical composition, antimicrobial and antioxidant properties of the volatile oil and methanol extract of *Xenophyllum poposum*. *Nat Prod Commun*. 2012;7(12):1934578X1200701230.
76. Li Y, Cao X, Sun J, et al. Characterization of chemical compositions by a GC-MS/MS approach and evaluation of antioxidant activities of essential oils from *Cinnamomum reticulatum* Hay, *Leptospermum petersonii* Bailey, and *Juniperus formosana* Hayata. *Arab J Chem*. 2022;15(2):103609. doi:10.1016/j.arabjc.2021.103609
77. Abutaha N. Apoptotic potential and chemical composition of Jordanian propolis extract against different cancer cell lines. *J Microbiol Biotechnol*. 2020;30(6):893. doi:10.4014/jmb.1905.05027
78. Farkas J, Mohácsi-Farkas C. Safety of food and beverages: spices and seasonings. In: Motarjemi Y, editor. *Encyclopedia of Food Safety*. Waltham: Academic Press; 2014:324–330.

79. Serabele K, Chen W, Combrinck S. Chapter 10 - Helichrysum odoratissimum. In: Viljoen A, Sandasi M, Fouche G, Combrinck S, Vermaak I, editors. *The South African Herbal Pharmacopoeia*. Academic Press; 2023:247–258.
80. Passos BG, de Albuquerque RDDG, Muñoz-Acevedo A, et al. Essential oils from *Ocotea* species: chemical variety, biological activities and geographic availability. *Fitoterapia*. 2022;156:105065. doi:10.1016/j.fitote.2021.105065
81. Adams M, Berset C, Kessler M, Hamburger M. Medicinal herbs for the treatment of rheumatic disorders—A survey of European herbals from the 16th and 17th century. *J Ethnopharmacol*. 2009;121(3):343–359. doi:10.1016/j.jep.2008.11.010
82. Lion Corp, assignee. Google patents: azulene anti-inflammatory agent (JPH0832626B2). 1996.
83. Guarrera M, Turbino L, Reborá A. The anti-inflammatory activity of azulene. *J European Acad Dermatol Venereol*. 2001;15(5):486–487. doi:10.1046/j.1468-3083.2001.00340.x
84. Bakun P, Czarczynska-Goslinska B, Goslinski T, Lijewski S. In vitro and in vivo biological activities of azulene derivatives with potential applications in medicine. *Med Chem Res*. 2021;30:834–846. doi:10.1007/s00044-021-02701-0
85. Martins FT, Doriguetto AC, de Souza TC, et al. Composition, and anti-inflammatory and antioxidant activities of the volatile oil from the fruit peel of *Garcinia brasiliensis*. *Chem Biodiver*. 2008;5(2):251–258. doi:10.1002/cbdv.200890022
86. Queiroz JCC, Antonioli ÁR, Quintans-Júnior LJ, et al. Evaluation of the anti-inflammatory and antinociceptive effects of the essential oil from leaves of *Xylopiá laevigata* in experimental models. *Sci World J*. 2014;2014:1–11. doi:10.1155/2014/816450
87. Satyavathi Chillumula JCP, Bramhanapalli M, Bhavani Nelavelli L. GC-MS metabolite profiling of bioactive compounds in leaf, fruit and seed extracts of *Syzygium cumini* (L.). *Int J Pharma Sci Res*. 2021;12(7):3814–3820.
88. Nadkarni K, Nadkarni A. Indian materia medica. *Bombay*. 1982;1:278–279.
89. Ahmed R, Tariq M, Hussain M, et al. Phenolic contents-based assessment of therapeutic potential of *Syzygium cumini* leaves extract. *PLoS One*. 2019;14(8):e0221318. doi:10.1371/journal.pone.0221318
90. Hosseinzadeh E, Foroumadi A, Firoozpour L. What is the role of phytochemical compounds as capping agents for the inhibition of aggregation in the green synthesis of metal oxide nanoparticles? A DFT molecular level response. *Inorg Chem Communi*. 2023;147:110243. doi:10.1016/j.inoche.2022.110243
91. Asmat-Campos D, Abreu AC, Romero-Cano MS, et al. Unraveling the active biomolecules responsible for the sustainable synthesis of nanoscale silver particles through nuclear magnetic resonance metabolomics. *ACS Sust Chem Engineer*. 2020;8(48):17816–17827. doi:10.1021/acssuschemeng.0c06903
92. Bandeira M, Possan AL, Pavin SS, et al. Mechanism of formation, characterization and cytotoxicity of green synthesized zinc oxide nanoparticles obtained from *Ilex paraguariensis* leaves extract. *Nano-Str Nano-Obj*. 2020;24:100532.
93. Ying S, Guan Z, Ofogebu PC, et al. Green synthesis of nanoparticles: current developments and limitations. *Environ Technol Innov*. 2022;26:102336. doi:10.1016/j.eti.2022.102336
94. Can M. Green gold nanoparticles from plant-derived materials: an overview of the reaction synthesis types, conditions, and applications. *Rev Chem Eng*. 2020;36(7):859–877. doi:10.1515/revce-2018-0051
95. Matinise N, Fuku X, Kaviyarasu K, Mayedwa N, Maaza M. ZnO nanoparticles via *Moringa oleifera* green synthesis: physical properties & mechanism of formation. *Appl Sur Sci*. 2017;406:339–347. doi:10.1016/j.apsusc.2017.01.219
96. Villagrán Z, Anaya-Esparza LM, Velázquez-Carriles CA, et al. Plant-based extracts as reducing, capping, and stabilizing agents for the green synthesis of inorganic nanoparticles. *Resources*. 2024;13(6):70. doi:10.3390/resources13060070
97. Zarzuela R, Luna MJ, Gil MLA, et al. Analytical determination of the reducing and stabilization agents present in different *Zostera noltii* extracts used for the biosynthesis of gold nanoparticles. *J Photochem Photobiol B*. 2018;179:32–38. doi:10.1016/j.jphotobiol.2017.12.025
98. Sharma D, Kanchi S, Bisetty K. Biogenic synthesis of nanoparticles: a review. *Arab J Chem*. 2019;12(8):3576–3600. doi:10.1016/j.arabjc.2015.11.002
99. Hammami I, Alabdallah NM, Jomaa AA, Kamoun M. Gold nanoparticles: synthesis properties and applications. *J King Saud Uni - Sci*. 2021;33(7):101560. doi:10.1016/j.jksus.2021.101560
100. Link S, Mohamed MB, El-Sayed M. Simulation of the optical absorption spectra of gold nanorods as a function of their aspect ratio and the effect of the medium dielectric constant. *J Phy Chem B*. 1999;103(16):3073–3077. doi:10.1021/jp990183f
101. Burrows ND, Lin W, Hinman JG, et al. Surface chemistry of gold nanorods. *Langmuir*. 2016;32(39):9905–9921. doi:10.1021/acs.langmuir.6b02706
102. Singh T, Jayaprakash A, Alsuwaidi M, Madhavan AA. Green synthesized gold nanoparticles with enhanced photocatalytic activity. *Mater Today*. 2021;42:1166–1169.
103. Srinath B, Ravishankar Rai V. Biosynthesis of highly monodispersed, spherical gold nanoparticles of size 4–10 nm from spent cultures of *Klebsiella pneumoniae*. *3 Biotech*. 2015;5:671–676. doi:10.1007/s13205-014-0265-2
104. Raza MA, Kanwal Z, Rauf A, Sabri AN, Riaz S, Naseem S. Size- and shape-dependent antibacterial studies of silver nanoparticles synthesized by wet chemical routes. *Nanomaterial*. 2016;6(4):74. doi:10.3390/nano6040074
105. Qian L, Su W, Wang Y, Dang M, Zhang W, Wang C. Synthesis and characterization of gold nanoparticles from aqueous leaf extract of *Alternanthera sessilis* and its anticancer activity on cervical cancer cells (HeLa). *Art Cell Nanomed Biotechnol*. 2019;47(1):1173–1180.
106. Anbu P, Gopinath SC, Jayanthi S. Synthesis of gold nanoparticles using *Platyodon grandiflorum* extract and its antipathogenic activity under optimal conditions. *Nanomater Nanotechnol*. 2020;10:1847980420961697. doi:10.1177/1847980420961697
107. Ahmad S, Ahmad S, Xu Q, et al. Green synthesis of gold and silver nanoparticles using crude extract of *Aconitum violaceum* and evaluation of their antibacterial, antioxidant and photocatalytic activities. *Front Bioengineer Biotechnol*. 2024;11:1320739. doi:10.3389/fbioe.2023.1320739
108. Abdullah JAA, Eddine LS, Abderrhmane B, Alonso-González M, Guerrero A, Romero A. Green synthesis and characterization of iron oxide nanoparticles by *Phoenix dactylifera* leaf extract and evaluation of their antioxidant activity. *Sustain Chem Pharma*. 2020;17:100280. doi:10.1016/j.scp.2020.100280
109. Lu J, Wang J-K. Agglomeration, breakage, population balance, and crystallization kinetics of reactive precipitation process. *Chem Engineer Commun*. 2006;193(7):891–902. doi:10.1080/00986440500267402
110. Vincent J, Lekha NC. Green synthesis of gold nanoparticles using *Pithecellobium dulce* leaf extract and its biological activities. *Chem Engineer Technol*. 2023;46:1424–1431. doi:10.1002/ceat.202100618

111. Bawazeer S, Khan I, Rauf A, et al. Black pepper (*Piper nigrum*) fruit-based gold nanoparticles (BP-AuNPs): synthesis, characterization, biological activities, and catalytic applications—A green approach. *Green Proce Syn*. 2022;11(1):11–28. doi:10.1515/gps-2022-0002
112. Yang Z, Liu Z, Zhu J, Xu J, Pu Y, Bao Y. Green synthesis and characterization of gold nanoparticles from *Pholiota adiposa* and their anticancer effects on hepatic carcinoma. *Drug Deliver*. 2022;29(1):997–1006. doi:10.1080/10717544.2022.2056664
113. Patel KN, Trivedi PG, Thakar MS, Prajapati KV, Prajapati DK, Sindhav GM. Gold nanoparticles synthesis using *Gymnosporia Montana* L. and its biological profile: a pioneer report. *J Genet Engineer Biotechnol*. 2023;21(1):71. doi:10.1186/s43141-023-00525-6
114. Song JY, Jang H-K, Kim BS. Biological synthesis of gold nanoparticles using *Magnolia kobus* and *Diopyros kaki* leaf extracts. *Process Biochem*. 2009;44(10):1133–1138. doi:10.1016/j.procbio.2009.06.005
115. Shah MZ, Guan Z-H, Din AU, et al. Synthesis of silver nanoparticles using *Plantago lanceolata* extract and assessing their antibacterial and antioxidant activities. *Sci Rep*. 2021;11(1):20754. doi:10.1038/s41598-021-00296-5
116. Abed AS, Khalaf YH, Mohammed AM. Green synthesis of gold nanoparticles as an effective opportunity for cancer treatment. *Result Chem*. 2023;5:100848. doi:10.1016/j.rechem.2023.100848
117. Mishra RC, Kalra R, Dilawari R, Goel M, Barrow CJ. Bio-synthesis of *Aspergillus terreus* mediated gold nanoparticle: antimicrobial, antioxidant, antifungal and in vitro cytotoxicity studies. *Material*. 2022;15(11):3877. doi:10.3390/ma15113877
118. XRD Crystallite (grain). Size calculator (Scherrer Equation) – InstaNANO; 2024. Available from: <https://instanano.com/all/characterization/xrd/crystallite-size/>. Accessed April 28, 2024.
119. Sneha K, Sathishkumar M, Kim S, Yun Y-S. Counter ions and temperature incorporated tailoring of biogenic gold nanoparticles. *Process Biochem*. 2010;45(9):1450–1458. doi:10.1016/j.procbio.2010.05.019
120. Krishnamurthy S, Esterle A, Sharma NC, Sahi SV. Yucca-derived synthesis of gold nanomaterial and their catalytic potential. *Nanoscale Res Lett*. 2014;9:1–9. doi:10.1186/1556-276X-9-627
121. Niranjan Dhanasekar N, Ravindran Rahul G, Badri Narayanan K, Raman G, Sakthivel N. Green chemistry approach for the synthesis of gold nanoparticles using the fungus *Alternaria* sp. *J Microbiol Biotechnol*. 2015;25(7):1129–1135. doi:10.4014/jmb.1410.10036
122. Sosa IO, Noguez C, Barrera RG. Optical properties of metal nanoparticles with arbitrary shapes. *J Phy Chem B*. 2003;107(26):6269–6275. doi:10.1021/jp0274076
123. Pochapski DJ, Carvalho Dos Santos C, Leite GW, Pulcinelli SH, Santilli CV. Zeta potential and colloidal stability predictions for inorganic nanoparticle dispersions: effects of experimental conditions and electrokinetic models on the interpretation of results. *Langmuir*. 2021;37(45):13379–13389. doi:10.1021/acs.langmuir.1c02056
124. Sharaf OZ, Taylor RA, Abu-Nada E. On the colloidal and chemical stability of solar nanofluids: from nanoscale interactions to recent advances. *Phys Rep*. 2020;867:1–84.
125. Singh H, Du J, Yi T-H. Green and rapid synthesis of silver nanoparticles using *Borago officinalis* leaf extract: anticancer and antibacterial activities. *Art Cell Nanomed Biotechnol*. 2017;45(7):1310–1316.
126. Sharma A, Sagar A, Rana J, Rani R. Green synthesis of silver nanoparticles and its antibacterial activity using fungus *Talaromyces purpureogenus* isolated from *Taxus baccata* Linn. *Micro Nano Syst Let*. 2022;10(1):1–12.
127. Carone A, Emilsson S, Mariani P, Désert A, Parola S. Gold nanoparticle shape dependence of colloidal stability domains. *Nanoscale Adv*. 2023;5(7):2017–2026. doi:10.1039/D2NA00809B
128. Coates J. Interpretation of infrared spectra, a practical approach. In: Meyers RA, editor. *Encyclopedia of Analytical Chemistry*. John Wiley & Sons Ltd.; 2000:24.
129. LibreTexts. Infrared Spectroscopy Absorption Table; 2024. Available from: https://chem.libretexts.org/Ancillary_Materials/Reference/Reference_Tables/Spectroscopic_Reference_Tables/Infrared_Spectroscopy_Absorption_Table. Accessed March 18, 2024.
130. Murali V, Devi VM. Antioxidant analysis, FTIR and GC-MS characterization of *Syzygium Cumini* leaf extract. *Annal Roman Soc Cell Biol*. 2021;15880–15892.
131. Kamaraj C, Karthi S, Reegan AD, et al. Green synthesis of gold nanoparticles using *Gracilaria crassa* leaf extract and their ecotoxicological potential: issues to be considered. *Environ Res*. 2022;213:113711. doi:10.1016/j.envres.2022.113711
132. Kasai D, Chougale R, Masti S, Chalannavar R, Malabadi RB, Gani R. Influence of *Syzygium cumini* leaves extract on morphological, thermal, mechanical, and antimicrobial properties of PVA and PVA/chitosan blend films. *J Appl Polym Sci*. 2018;135(17):46188. doi:10.1002/app.46188
133. Siddig M, Abdelgadir E, Elbadawi A, Mustafal M, Mussa A. Structural characterization and physical properties of *Syzygium cumini* flowering plant. *Int J Innov Res Sci Eng*. 2015;4:2694.
134. Patra JK, Baek K-H. Comparative study of proteasome inhibitory, synergistic antibacterial, synergistic anticandidal, and antioxidant activities of gold nanoparticles biosynthesized using fruit waste materials. *Int J Nanomed*. 2016;11:4691. doi:10.2147/IJN.S108920
135. Hamelian M, Varmira K, Veisi H. Green synthesis and characterizations of gold nanoparticles using thyme and survey cytotoxic effect, antibacterial and antioxidant potential. *J Photochem Photobiol B*. 2018;184:71–79. doi:10.1016/j.jphotobiol.2018.05.016
136. Ismail EH, Saqer AM, Assirey E, Naqvi A, Okasha RM. Successful green synthesis of gold nanoparticles using a *Corchorus olitorius* extract and their antiproliferative effect in cancer cells. *Int J Mol Sci*. 2018;19(9):2612. doi:10.3390/ijms19092612
137. Younis HM, Hussein HA, Khaphi FL, Saeed ZK. Green biosynthesis of silver and gold nanoparticles using teak (*Tectona grandis*) leaf extract and its anticancer and antimicrobial activity. *Heliyon*. 2023;9(11):e21698. doi:10.1016/j.heliyon.2023.e21698
138. Sikkema J, de Bont JA, Poolman B. Interactions of cyclic hydrocarbons with biological membranes. *J Biol Chem*. 1994;269(11):8022–8028. doi:10.1016/S0021-9258(17)37154-5
139. Rai A, Prabhune A, Perry CC. Antibiotic mediated synthesis of gold nanoparticles with potent antimicrobial activity and their application in antimicrobial coatings. *J Mat Chem*. 2010;20(32):6789–6798. doi:10.1039/c0jm00817f
140. Zivanovic S, Chi S, Draughon AF. Antimicrobial activity of chitosan films enriched with essential oils. *J Food Sci*. 2005;70(1):M45–M51. doi:10.1111/j.1365-2621.2005.tb09045.x
141. Singh JP, Kaur A, Singh N, et al. In vitro antioxidant and antimicrobial properties of jambolan (*Syzygium cumini*) fruit polyphenols. *LWT-Food Sci Technol*. 2016;65:1025–1030. doi:10.1016/j.lwt.2015.09.038
142. Imran M, Imran M, Khan S. Antibacterial activity of *Syzygium cumini* leaf extracts against multidrug resistant pathogenic bacteria. *J Appl Pharm Sci*. 2017;7(3):168–174.

143. Oliveira G, Furtado NAJC, Silva Filho A, et al. Antimicrobial activity of *Syzygium cumini* (Myrtaceae) leaves extract. *Braz J Microbiol.* 2007;38:381–384. doi:10.1590/S1517-83822007000200035
144. Franzolin MR, Courrol D, Silva F, Courrol LC. Antimicrobial activity of silver and gold nanoparticles prepared by photoreduction process with leaves and fruit extracts of *Plinia cauliflora* and *Punica granatum*. *Molecules.* 2022;27(20):6860. doi:10.3390/molecules27206860
145. Folorunso A, Akintelu S, Oyebamiji AK, et al. Biosynthesis, characterization and antimicrobial activity of gold nanoparticles from leaf extracts of *Annona muricata*. *J Nanostr Chem.* 2019;9:111–117. doi:10.1007/s40097-019-0301-1
146. Chandraker SK, Kumar R. Biogenic biocompatible silver nanoparticles: a promising antibacterial agent. *Biotechnol Gene Engineer Rev.* 2022;1–35.
147. Rokkarukala S, Cherian T, Ragavendran C, et al. One-pot green synthesis of gold nanoparticles using *Sarcophyton crassocaule*, a marine soft coral: assessing biological potentialities of antibacterial, antioxidant, anti-diabetic and catalytic degradation of toxic organic pollutants. *Heliyon.* 2023;9(3):e14668. doi:10.1016/j.heliyon.2023.e14668
148. Manna K, Mishra S, Saha M, et al. Amelioration of diabetic nephropathy using pomegranate peel extract-stabilized gold nanoparticles: assessment of NF- κ B and Nrf2 signaling system. *Int J Nanomed.* 2019;14:1753–1777. doi:10.2147/IJN.S176013
149. Yu Y, Gao J, Jiang L, Wang J. Antidiabetic nephropathy effects of synthesized gold nanoparticles through mitigation of oxidative stress. *Arab J Chem.* 2021;14(3):103007. doi:10.1016/j.arabjc.2021.103007
150. Ramachandran V, Arokia Vijaya Anand M, David E, et al. Antidiabetic activity of gold nanoparticles synthesized using wedelolactone in RIN-5F cell line. *Antioxidant.* 2019;9(1):8. doi:10.3390/antiox9010008
151. Asam Raza M, Farwa U, Waseem Mumtaz M, Kainat J, Sabir A, Al-Sehemi AG. Green synthesis of gold and silver nanoparticles as antidiabetic and anticancerous agents. *Green Chem Lett Rev.* 2023;16(1):2275666. doi:10.1080/17518253.2023.2275666
152. Bakshi A, Sharma N, Nagpal AK. Comparative evaluation of in vitro antioxidant and antidiabetic potential of five ethnomedicinal plant species from Punjab, India. *South Afr J Bot.* 2022;150:478–487. doi:10.1016/j.sajb.2022.08.019
153. Poongunran J, Perera HKI, Jayasinghe L, et al. Bioassay-guided fractionation and identification of α -amylase inhibitors from *Syzygium cumini* leaves. *Pharma Biol.* 2017;55(1):206–211. doi:10.1080/13880209.2016.1257031
154. Bhavi SM, Mirji SK, Thokchom B, et al. Potential antidiabetic properties of *Syzygium Cumini* (L.) Skeels leaf extract-mediated silver nanoparticles. *Austin J Anal Pharm Chem.* 2024;11(1):1–7.
155. Lima RM, Polonini HC, Brandão MA, Raposo FJ, Raposo NR, Dutra RC. In vitro assessment of anti-aging properties of *Syzygium cumini* (L.) leaves extract. *Biomed J Sci Tech Res.* 2019;13(4):10185–10191.
156. Rizzi V, Gubitosa J, Fini P, Nuzzo S, Agostiano A, Cosma P. Snail slime-based gold nanoparticles: an interesting potential ingredient in cosmetics as an antioxidant, sunscreen, and tyrosinase inhibitor. *J Photochem Photobiol B.* 2021;224:112309. doi:10.1016/j.jphotobiol.2021.112309
157. Gubitosa J, Rizzi V, Fini P, et al. Multifunctional green synthesized gold nanoparticles/chitosan/ellagic acid self-assembly: antioxidant, sun filter and tyrosinase-inhibitor properties. *Mat Sci Engineer C.* 2020;106:110170. doi:10.1016/j.msec.2019.110170
158. Tettey C, Nagajyothi P, Lee S, et al. Anti-melanoma, tyrosinase inhibitory and anti-microbial activities of gold nanoparticles synthesized from aqueous leaf extracts of *Teraxacum officinale*. *Int J Cosmet Sci.* 2012;34(2):150–154. doi:10.1111/j.1468-2494.2011.00694.x
159. Cui H-X, Duan -F-F, Jia -S-S, Cheng F-R, Yuan K. Antioxidant and tyrosinase inhibitory activities of seed oils from *Torreya grandis* Fort. ex Lindl. *BioMed Res Int.* 2018;2018:1–10. doi:10.1155/2018/5314320
160. Alam N, Yoon KN, Lee JS, Cho HJ, Lee TS. Consequence of the antioxidant activities and tyrosinase inhibitory effects of various extracts from the fruiting bodies of *Pleurotus ferulae*. *Saudi J Biol Sci.* 2012;19(1):111–118. doi:10.1016/j.sjbs.2011.11.004
161. Panzella L, Napolitano A. Natural and bioinspired phenolic compounds as tyrosinase inhibitors for the treatment of skin hyperpigmentation: recent advances. *Cosmetic.* 2019;6(4):57. doi:10.3390/cosmetics6040057
162. Ruan ZP, Zhang LL, Lin YM. Evaluation of the antioxidant activity of *Syzygium cumini* leaves. *Molecule.* 2008;13(10):2545–2556. doi:10.3390/molecules13102545
163. Eshwarappa RSB, Iyer RS, Subbaramaiah SR, Richard SA, Dhananjaya BL. Antioxidant activity of *Syzygium cumini* leaf gall extracts. *Bioimpacts.* 2014;4(2):101. doi:10.5681/bi.2014.018
164. Decker EA. Phenolics: prooxidants or antioxidants? *Nutrition Rev.* 1997;55(11):396–398. doi:10.1111/j.1753-4887.1997.tb01580.x
165. Rice-evans CA, Miller NJ, Bolwell PG, Bramley PM, Pridham JB. The relative antioxidant activities of plant-derived polyphenolic flavonoids. *Free Radical Res.* 1995;22(4):375–383. doi:10.3109/10715769509145649
166. Dehghani F, Mosleh-Shirazi S, Shafiee M, Kasaei SR, Amani AM. Antiviral and antioxidant properties of green synthesized gold nanoparticles using *Glaucium flavum* leaf extract. *Appl Nanosci.* 2023;13(6):4395–4405. doi:10.1007/s13204-022-02705-1
167. Elsabahy M, Wooley KL. Cytokines as biomarkers of nanoparticle immunotoxicity. *Chem Soc Rev.* 2013;42(12):5552–5576. doi:10.1039/c3cs60064e
168. Allenspach M, Steuer C. α -Pinene: a never-ending story. *Phytochem.* 2021;190:112857. doi:10.1016/j.phytochem.2021.112857
169. Saldanha E, Pai RJ, George T, et al. Chapter 17 - health effects of various dietary agents and phytochemicals (therapy of acute pancreatitis). In: Grumezescu AM, Holban AM, editors. *Therapeutic, Probiotic, and Unconventional Foods*. Academic Press; 2018:303–314.
170. Nabeta K, Kigure K, Fujita M, et al. Biosynthesis of (+)-cubenene and (+)-epicubenol by cell-free extracts of cultured cells of *Heteroscyphus planus* and cyclization of [2H] farnesyl diphosphates. *J Chem Soc Perkin Transact 1.* 1995;1(15):1935–1939. doi:10.1039/p19950001935
171. Chen C, Yao G, Wang F, et al. Identification of a (+)-cubenene synthase from filamentous fungi *Acremonium chrysogenum*. *Biochem Biophys Res Comm.* 2023;677:119–125. doi:10.1016/j.bbrc.2023.08.018
172. Rădulescu M, Jianu C, Lukinich-Gruia AT, et al. Chemical composition, in vitro and in silico antioxidant potential of *Melissa officinalis* subsp. *officinalis* essential oil. *Antioxidants.* 2021;10(7):1081. doi:10.3390/antiox10071081
173. Xu W, Popovich DG. Chapter 3 - bioactive hybrid compounds from Myrtaceae: chemical classification and biological activities. In: Atta Ur R, editor. *Studies in Natural Products Chemistry*. Vol. 77. Elsevier; 2023:65–109.
174. Russo EB, Marcu J. Chapter three - cannabis pharmacology: the usual suspects and a few promising leads. In: Kendall D, Alexander SPH, editors. *Advances in Pharmacology*. Vol. 80. Academic Press; 2017:67–134.
175. Abbas Q, Saleem M, Phull AR, et al. Green synthesis of silver nanoparticles using *Bidens frondosa* extract and their tyrosinase activity. *Iran J Pharm Res.* 2017;16(2):763.
176. Singh RK, Behera SS, Singh KR, et al. Biosynthesized gold nanoparticles as photocatalysts for selective degradation of cationic dye and their antimicrobial activity. *J Photochem Photobiol A.* 2020;400:112704. doi:10.1016/j.jphotochem.2020.112704

177. Steffi AM, Hyam RS. Au nanoparticles decorated titanium dioxide nanotube arrays with enhanced photocatalytic dye degradation under ultraviolet and sunlight irradiation. *Result Sur Interface*. 2023;12:100140. doi:10.1016/j.rsufi.2023.100140
178. León ER, Rodríguez EL, Beas CR, Plascencia-Villa G, Palomares RAI. Study of methylene blue degradation by gold nanoparticles synthesized within natural zeolites. *J Nanomater*. 2016;2016:1–10. doi:10.1155/2016/9541683
179. Mondal S, Reyes MEDA, Pal U. Plasmon induced enhanced photocatalytic activity of gold loaded hydroxyapatite nanoparticles for methylene blue degradation under visible light. *RSC Adv*. 2017;7(14):8633–8645. doi:10.1039/C6RA28640B
180. Lu J, Batjikh I, Hurr J, et al. Photocatalytic degradation of methylene blue using biosynthesized zinc oxide nanoparticles from bark extract of *Kalopanax septemlobus*. *Optik*. 2019;182:980–985. doi:10.1016/j.ijleo.2018.12.016
181. Ahmed SN, Haider W. Heterogeneous photocatalysis and its potential applications in water and wastewater treatment: a review. *Nanotechnol*. 2018;29(34):342001. doi:10.1088/1361-6528/aac6ea
182. Das G, Seo S, Yang I-J, Nguyen LTH, Shin H-S, Patra JK. Sericin mediated gold/silver bimetallic nanoparticles and exploration of its multi-therapeutic efficiency and photocatalytic degradation potential. *Environ Res*. 2023;229:115935. doi:10.1016/j.envres.2023.115935
183. Chandrasekar A, Vasantharaj S, Jagadeesan NL, et al. Studies on phytochemical mediated synthesis of copper oxide nanoparticles for biomedical and environmental applications. *Biocat Agri Biotechnol*. 2021;33:101994. doi:10.1016/j.bcab.2021.101994
184. Li X, Hou Y, Zhao Q, Wang L. A general, one-step and template-free synthesis of sphere-like zinc ferrite nanostructures with enhanced photocatalytic activity for dye degradation. *J Colloid Int Sci*. 2011;358(1):102–108. doi:10.1016/j.jcis.2011.02.052
185. Ahluwalia S, Prakash NT, Prakash R, Pal B. Improved degradation of methyl Orange dye using bio-co-catalyst Se nanoparticles impregnated ZnS photocatalyst under UV irradiation. *Chem Engr J*. 2016;306:1041–1048. doi:10.1016/j.cej.2016.08.028
186. Gao X, Yin H, Guo C, et al. Comprehensive removal of various dyes by thiourea modified chitosan/nano ZnS composite via enhanced photocatalysis: performance and mechanism. *Int J Biol Macromol*. 2023;247:125677. doi:10.1016/j.ijbiomac.2023.125677
187. Thakare Y, Kore S, Sharma I, Shah M. A comprehensive review on sustainable greener nanoparticles for efficient dye degradation. *Environ Sci Poll Res*. 2022;29(37):55415–55436. doi:10.1007/s11356-022-20127-y
188. Saeed M, Usman M, Haq A. Catalytic degradation of organic dyes in aqueous medium. *IntechOpen*. 2018;13:197.
189. Appavu B, Thiripuranthagan S, Ranganathan S, Erusappan E, Kannan K. BiVO₄/N-rGO nano composites as highly efficient visible active photocatalyst for the degradation of dyes and antibiotics in eco system. *Ecotoxicol Environ Safe*. 2018;151:118–126. doi:10.1016/j.ecoenv.2018.01.008
190. Riaz T, Munnwar A, Shahzadi T, et al. Phyto-mediated synthesis of nickel oxide (NiO) nanoparticles using leaves' extract of *Syzygium cumini* for antioxidant and dyes removal studies from wastewater. *Inorgan Chem Commun*. 2022;142:109656. doi:10.1016/j.inoche.2022.109656
191. Brillas E, Martínez-Huitle CA. Decontamination of wastewaters containing synthetic organic dyes by electrochemical methods. An updated review. *Appl Catal B Environ*. 2015;166:603–643. doi:10.1016/j.apcatb.2014.11.016
192. Vasiljevic Z, Dojcinovic M, Vujanecvic J, et al. Photocatalytic degradation of methylene blue under natural sunlight using iron titanate nanoparticles prepared by a modified sol–gel method. *R Soc Open Sci*. 2020;7(9):200708. doi:10.1098/rsos.200708
193. Chokkalingam M, Jahan Rupa E, Huo Y, et al. Photocatalytic degradation of industrial dyes using Ag and Au nanoparticles synthesized from *Angelica gigas* ribbed stem extracts. *Optik*. 2019;185:1213–1219. doi:10.1016/j.ijleo.2019.04.065
194. Baruah D, Goswami M, Yadav RNS, Yadav A, Das AM. Biogenic synthesis of gold nanoparticles and their application in photocatalytic degradation of toxic dyes. *J Photochem Photobiol B*. 2018;186:51–58. doi:10.1016/j.jphotobiol.2018.07.002

International Journal of Nanomedicine

Dovepress

Publish your work in this journal

The International Journal of Nanomedicine is an international, peer-reviewed journal focusing on the application of nanotechnology in diagnostics, therapeutics, and drug delivery systems throughout the biomedical field. This journal is indexed on PubMed Central, MedLine, CAS, SciSearch®, Current Contents®/Clinical Medicine, Journal Citation Reports/Science Edition, EMBase, Scopus and the Elsevier Bibliographic databases. The manuscript management system is completely online and includes a very quick and fair peer-review system, which is all easy to use. Visit <http://www.dovepress.com/testimonials.php> to read real quotes from published authors.

Submit your manuscript here: <https://www.dovepress.com/international-journal-of-nanomedicine-journal>